Astron. Astrophys. 154, 25–41 (1986)

ASTRONOMY AND ASTROPHYSICS

The radial distribution of galactic gamma rays

III. The distribution of cosmic rays in the Galaxy and the CO-H_2 calibration

J.B.G.M. Bloemen [1,9,10], A.W. Strong [4], L. Blitz [7,9,⋆], R.S. Cohen [8], T.M. Dame [8], D.A. Grabelsky [8], W. Hermsen [1], F. Lebrun [5], H.A. Mayer-Hasselwander [4], and P. Thaddeus [8]

The Caravane Collaboration for the COS-B satellite:
[1] Laboratory for Space Research Leiden, Leiden, The Netherlands
[2] Istituto di Fisica Cosmica del CNR, Milano, Italy
[3] Istituto di Fisica Cosmica e Informatica del CNR, Palermo, Italy
[4] Max-Planck-Institut für Physik und Astrophysik, Institut für Extraterrestrische Physik, Garching, Federal Republic of Germany
[5] Service d'Astrophysique, Centre d'Etudes Nucléaires de Saclay, Gif-sur-Yvette, France
[6] Space Science Department of the European Space Agency, ESTEC, Noordwijk, The Netherlands
and:
[7] Astronomy Program, University of Maryland, College Park, USA
[8] Goddard Institute for Space Studies and Columbia University, New York, USA
9 Sterrewacht Leiden, Huygens Laboratorium, Leiden, The Netherlands
[10] Astronomy Department, University of California, Berkeley, CA94720, USA

Received May 15, accepted August 9, 1985

Summary. High-energy (>70 MeV) gamma-ray observations are compared to H I and CO surveys over more than half of the Milky Way. The kinematics of both H I and CO are used as a distance indicator to determine, in combination with COS-B gamma-ray data, the galacto-centric distribution of the gamma-ray emissivity (the production rate per H atom) for three gamma-ray energy intervals. The ratio between H_2 column density and integrated CO line intensity is calibrated independently of excitation and abundance effects. The galacto-centric distributions of cosmic-ray electrons and nuclei are derived separately from the gamma-ray emissivity distributions.

For each energy range the gamma-ray emissivity increases towards the inner parts of the Galaxy, but the near constancy of the high-energy (300 MeV–5 GeV) emissivity beyond the solar circle out to large distances [discussed in Paper II (Bloemen et al., 1984c)] remains valid; the gradient is strongest for low energies (70–150 MeV). The corresponding galacto-centric cosmic-ray distributions are shown to be described satisfactorily by exponential distributions for $R \gtrsim 3$ kpc ($R_\odot = 10$ kpc), with a radial scale length of 4–11 kpc for electrons (with energies up to several hundreds of MeV) and a scale length >18 kpc for nuclei (with energies of a few GeV). Although a cosmic-ray electron gradient is required to explain the observations, the results are consistent with a constant density of cosmic-ray nuclei throughout the entire Galaxy. These cosmic-ray gradients are upper limits if a population of unresolved galactic gamma-ray sources exists with a latitude distribution similar to that of the gas, but with a stronger concentration towards the inner parts of the Galaxy. Previous studies that indicated a strong density gradient for cosmic-ray nuclei in the outer Galaxy, first claimed by Dodds et al. (1975), are shown to be incorrect.

On a large scale, the ratio between molecular-hydrogen column density and integrated CO line intensity is found to be constant throughout the Galaxy, within uncertainties. Our estimate of this ratio is $N(H_2)/W_{CO} = 2.8\ 10^{20}$ mol·cm^{-2}K^{-1} km^{-1}s, although, due to systematic effects, the true value is likely to be lower. The resultant H_2 mass is found to be equal to the H I mass for 2 kpc < R < 10 kpc.

Key words: cosmic rays – gamma rays – interstellar medium: molecules: CO – COS-B

Send offprint requests to: J.B.G.M. Bloemen (American address)

⋆ Alfred P. Sloan Foundation Fellow

1. Introduction

Gamma-ray astronomy offers an excellent means to study the distribution of cosmic-ray (CR) particles throughout the Galaxy. The diffuse component of the galactic high-energy ($\gtrsim$50 MeV) gamma rays results mainly from the interaction of CR nuclei and electrons with the nuclei of the interstellar gas (via the decay of π^0-mesons and bremsstrahlung, respectively) and from the interaction of CR electrons with interstellar photons through the inverse-Compton (IC) process. For a review of the various production mechanisms see Fazio (1967) and Stecker (1971). The numerous gamma-ray studies of the CR distribution performed in the past, using gamma-ray observations obtained by the SAS-2 and COS-B satellites, suffered severely from uncertainties in the galactic distribution of interstellar molecular hydrogen. Large-scale millimetre surveys of the CO molecule covering more than half of the Milky Way are currently available and can be used to trace the H_2, and the COS-B observations used in this paper have sufficient resolution and sensitivity to determine the relation between the integrated CO line intensity and the molecular-hydrogen column density $N(H_2)$ (Lebrun et al., 1983; Bloemen et al., 1984a). While most previous studies were based on longitude and latitude profiles

integrated over large parts of the sky, or on radial unfoldings of the data, we use all the structure in the various observations as far as possible.

Using COS-B data, Bloemen et al. (1984b, c; hereafter referred to as Papers I and II) showed that the gamma-ray intensity in the second and third galactic quadrants can generally be explained by CR interactions with the atomic-hydrogen alone (that is, H_2 can be neglected within the uncertainties of the analysis). The galacto-centric distribution of the gamma-ray emissivity (the production rate per H atom), which is proportional to the CR density, was determined for three energy ranges (70–150 MeV, 150–300 MeV, and 300 MeV–5 GeV) from a correlation study of the H I column density $N(\mathrm{H\,I})$ and gamma-ray intensity, using the velocity information of the H I 21-cm line as a distance indicator. The spectral shape of the gamma radiation due to the CR nuclei interactions (the π^0-decay spectrum, with a maximum at ~ 68 MeV) differs from the shape of the gamma rays produced by the CR-electron interactions (primarily bremsstrahlung, characterized by a spectrum that decreases monotonically with energy) (see e.g. Stecker, 1971), so the spatial distribution of the gamma-ray emissivity spectrum could be used to trace CR electrons and nuclei separately. The gamma-ray emissivity for the 70–150 MeV range (which has a large electron-bremsstrahlung contribution) was found to decrease in the outer Galaxy. This decrease was interpreted as a negative galacto-centric gradient in the distribution of the CR electron density for electrons with energies below ~ 300 MeV, as has been advocated for some years. By contrast, the gamma-ray emissivity for the 300 MeV–5 GeV range (dominated by π^0-decay) was found to be approximately constant and equal to the local value out to large (~ 20 kpc) galacto-centric distances. This finding was interpreted as a near constancy (within $\sim 20\,\%$) of the density of CR nuclei with energies of a few GeV out to large distances.

This paper extends the determination of the CR distribution to regions inside the solar circle by using the kinematics of both H I and CO to ascertain the spatial distribution of the interstellar gas. The conversion factor between integrated CO line intensity and $N(H_2)$ is determined. In addition, possible large-scale variations of this relationship throughout the Galaxy are investigated. Until now, such a complete and internally consistent approach has not been possible.

2. Method and data

2.1. *Outline of the model*

Assuming circular motions, the galacto-centric distance R of the H I and CO emission can be directly related to the radial velocity v_r of the features in the observed spectra (relative to the LSR), following the well-known relation $v_r = (w - w_\odot) R_\odot \sin l$, where $w = \theta/R$ and $\theta(R)$ represents the rotation curve of the Galaxy. $R_\odot$ was taken to be 10 kpc. To determine distances in the outer Galaxy ($R > R_\odot$), we used the rotation curve given by Blitz et al. (1980) as modified by Kulkarni et al. (1982); the curve of Burton and Gordon (1978) was used to determine distances for $R < R_\odot$. Maps of the H I column densities were constructed in four galacto-centric distance ranges: $2\,\mathrm{kpc} < R < 8\,\mathrm{kpc}$, $8\,\mathrm{kpc} < R < 10\,\mathrm{kpc}$, $10\,\mathrm{kpc} < R < 15\,\mathrm{kpc}$, and $R > 15\,\mathrm{kpc}$. Similarly, the CO spectra were integrated over the velocity intervals (yielding a quantity hereafter referred to as W_{CO}) which correspond to the same distance intervals as for H I (a detailed discussion of the construction of these maps is given in Sect. 2.2). For comparison with the gamma-ray observations, the maps were convolved with the energy-dependent COS-B point-spread function (Hermsen, 1980).

Ascertaining the contribution of the gas in each distance range to the observed gamma-ray intensities requires distinct differences among the angular distributions of the gas in each distance interval; the gas content of the Galaxy was therefore divided into four distance ranges, for which such differences exist (see Figs. 1 and 2). Similarly, to determine the conversion factor between W_{CO} and H_2 column density throughout the Galaxy [i.e. the ratio $X \equiv N(H_2)/W_{CO}$] requires distinct differences between the structures in the H I and CO maps. Last, the limited counting statistics of the COS-B data base restricted us to only a few distance intervals. See Paper II for a description of the gamma-ray data base used.

We assumed that the observed skymaps of gamma-ray intensities $I_{\gamma,j}$ in three energy intervals ($j = 1, 2, 3$ corresponds to the 70–150 MeV, 150 MeV–300 MeV, and 300 MeV–5 GeV ranges), can be represented by a relation of the form:

$$I_{\gamma,j} = \left\{ \sum_{i=1}^{4} \frac{q_{ij}}{4\pi} \cdot [N(\mathrm{H\,I})_{ij} + 2\,Y_{ij} \cdot W_{\mathrm{CO},ij}] \right\} + I_{\mathrm{IC},j} + I_{b,j}. \quad (1)$$

The index $i = 1, 2, 3, 4$ corresponds to the four distance intervals $R = 2$–8 kpc, $R = 8$–10 kpc, $R = 10$–15 kpc, and $R > 15$ kpc. $N(\mathrm{H\,I})_{ij}$ and $W_{\mathrm{CO},ij}$ are the convolved maps of the H I column densities and CO intensities for each distance interval i and each energy interval j. The term enclosed by braces represents the gamma-ray intensities that originate from CR collisions with atomic and molecular hydrogen. The term $I_{\mathrm{IC},j}$ represents the inverse-Compton contribution to the observed gamma-ray intensities (described in Sect. 2.3). $I_{b,j}$ is the total isotropic gamma-ray background, including the (dominant) instrumental background. The parameters q_{ij} are the gamma-ray emissivities. The parameters Y_{ij} are related to the ratio X for each distance interval (X_i) by the relation

$$Y_{ij} = \frac{q_{ij}(H_2)}{q_{ij}} \cdot X_i, \quad (2)$$

where $q_{ij}(H_2)$ is the emissivity of the gamma rays associated with H_2. The ratio $q_{ij}(H_2)/q_{ij}$, which allows for a possible exclusion of CR particles from, or concentration in molecular clouds, was assumed to be constant throughout the Galaxy ($q_{1j}(H_2)/q_{1j} = q_{2j}(H_2)/q_{2j} = \ldots$), equivalent to the assumption that the CR penetration is the same for all clouds. If the gamma-ray emissivity is uniform inside a certain distance interval i ($q_{ij}(H_2)/q_{ij} = 1$), then Y_{ij} equals X_i, independent of energy. On the other hand, different Y_{ij} values as a function of energy may indicate that the spectrum of the gamma-ray emission from the atomic hydrogen is different from that from the molecular. However, the interpretation of Y_{ij} is not unique; for example in the case of a population of unresolved galactic gamma-ray sources distributed like CO, Y_{ij} would be an overestimate of X_i (for discussion on this point see Sect. 5).

2.2. *CO and* H I *data*

The portion of the Milky Way included in the analysis is limited by the coverage of the sky in the currently available CO surveys. The COS-B gamma-ray survey and the Berkeley and Parkes H I surveys cover essentially the entire galactic plane, extending in latitude at least several tens of degrees. The most complete CO surveys, done with the Columbia 1.2-m millimetre-wave telescopes in New York and Cerro Tololo (Chile), provide longitude coverage for nearly the entire first galactic quadrant ($l > 11°.5$; Dame and Thaddeus,

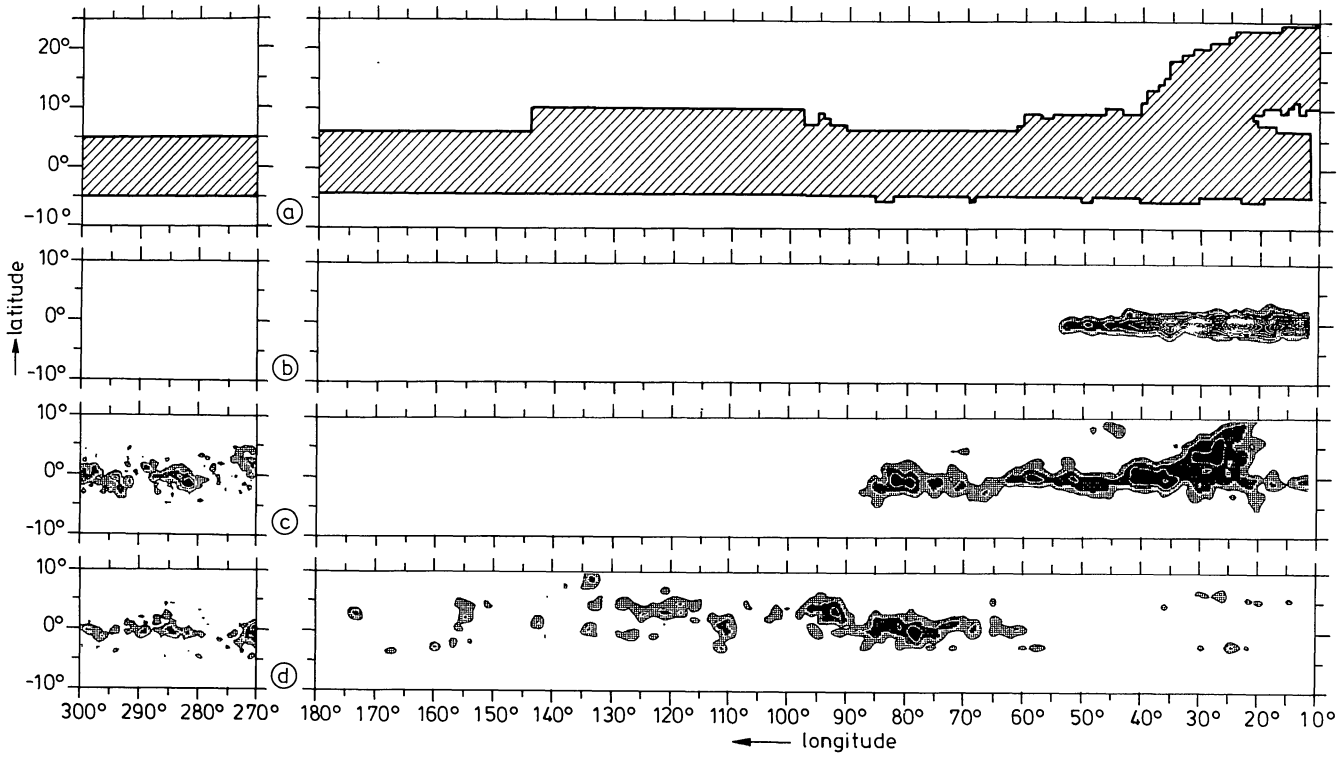

Fig. 1a–d. Sky coverage of the CO observations of the first and second galactic quadrants and of the Carina region used in this paper (**a**) and CO intensities for the galacto-centric distance intervals 2 kpc $< R <$ 8 kpc (**b**), 8 kpc $< R <$ 10 kpc (**c**), and $R >$ 10 kpc (**d**). Contour values: 4, 8, 15, 25, 35, ... K kms^{-1}

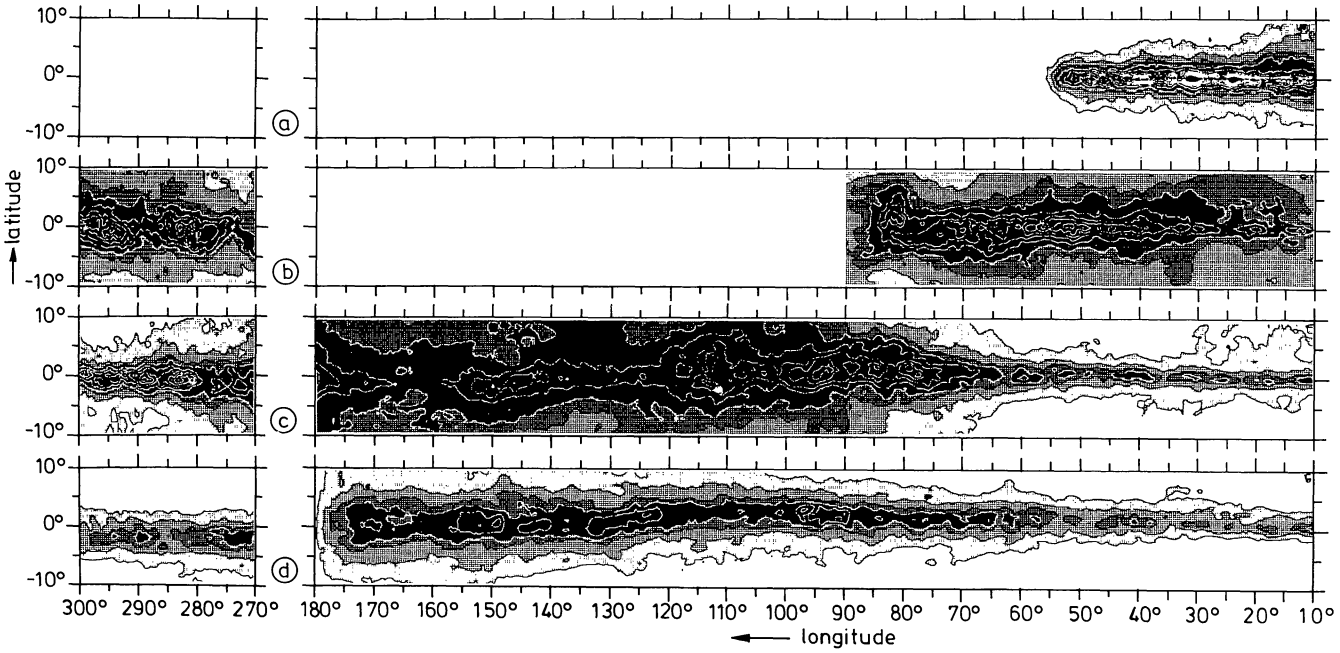

Fig. 2a–d. H I column-density maps of the first and second galactic quadrants and of the Carina region for the galacto-centric distance intervals 2 kpc $< R <$ 8 kpc (**a**), 8 kpc $< R <$ 10 kpc (**b**), 10 kpc $< R <$ 15 kpc (**c**), and $R >$ 15 kpc (**d**). Contour values: (0.4, 1, 2, 3, 5, 7, ...) 10^{21} H atom cm^{-2}

1985), for the entire second quadrant (Brock et al., 1985), and for the Carina region ($270° < l < 300°$; Cohen et al., 1985a). The coverage in latitude is essentially complete from $b = -4°.5$ to $b = +6°.5$, with several extensions to higher latitudes, particularly in the longitude range $8° \lesssim l \lesssim 40°$ (Lebrun and Huang, 1984). The sky coverage of the CO observations used in the present work is shown in Fig. 1a. The angular resolution of the Columbia CO surveys (1° in the first quadrant, $-5°.5 < b < 10°.5$, and 0°.5 elsewhere) is adequate for comparison with available gamma-ray data.

The sky maps of W_{CO} for three distance intervals are shown in Fig. 1 b–d (the maps for $R > 15$ kpc and 10 kpc $< R <$ 15 kpc were combined, because the amount of CO outside 15 kpc is very small). When these maps were convolved with the COS-B point-spread function, zero values were assumed outside the latitude band mapped in CO. The error introduced is probably small, because the average CO intensities at higher latitudes are negligible compared to those at low latitudes. Furthermore, the analysis in the present work will be restricted to a fairly small latitude range and the impact of possible CO concentrations at higher latitudes is expected to be small. This expectation will be verified *a posteriori*.

The H I surveys of Weaver and Williams (1973; $|b| < 10°$) and Heiles and Habing (1974; $|b| > 10°$) were used to obtain H I column densities for the four distance intervals in the first and second galactic quadrants. In the Carina region, the surveys of Strong et al. (1982a; $|b| < 10°$) and Heiles and Cleary (1979; $|b| > 10°$) were used. The H I column density was derived as in Papers I and II. The resultant column-density maps are shown in Fig. 2 for a limited latitude range; the high-latitude surveys were used to obtain the contribution to the convolved maps from $|b| > 10°$.

2.3. *The inverse-Compton model*

The IC gamma-ray intensities $I_{IC,j}$ for each energy range j, which originate from the interaction between CR electrons (with energies >1 GeV) and interstellar photons (mainly in the optical and infrared range), were estimated from the work of Bloemen (1985). An electron scale height of 750 pc was adopted. The radial distribution of the CR electrons, a topic studied in this paper (Sect. 4), was estimated in an iterative manner; to obtain the final results presented in this paper, the electron density in the 2–8 kpc range was assumed to be twice the local value (see Sect. 4) in determining the IC intensities. In any event, near the galactic plane the IC contribution predicted by this model does not, in general, exceed 5% for the three energy ranges, as shown by Bloemen for different electron distribution models (including the model favoured by the present work). The uncertainties in the IC estimates therefore have no significant impact on our results.

2.4. *The fitting procedure*

We applied a likelihood analysis, similar to that used in Paper II, on $1° \times 1°$ bins to determine the values of the parameters q_{ij}, Y_{ij}, and $I_{b,j}$ ($i = 1, 2, 3, 4$; $j = 1, 2, 3$). The formal uncertainties of the parameters were determined from the distribution of the likelihood ratio λ for each parameter, defining the λ-value which corresponds to a certain value of each parameter as the ratio between the likelihood maximized over the remaining parameters and the likelihood maximized over all parameters (see e.g. Eadie et al., 1971). Since in this case the quantity $-2 \ln \lambda$ has a chi-square distribution with 1 degree of freedom (Eadie et al.), the 68% confidence level corresponds to $-2 \ln \lambda = 1.0$, the 95% level to $-2 \ln \lambda = 3.8$, etc.

The sky area that can be used in the fitting procedure being limited by the coverage of the CO observations and, further, by uncertainties in the convolution at the edges of the CO survey, we restricted ourselves to the latitude range $-4°.5 < b < 6°.5$ and the longitude ranges $14°.5 < l < 165°.5$ and $270°.5 < l < 299°.5$. The cut-off at $l = 165°.5$ avoids the use of unreliable kinematic distances in the anti-centre region. In principle, the third galactic quadrant and higher-latitude regions (for which only H I surveys are available) might be included because the H_2 contribution is expected to be small, but we prefer to avoid systematic errors that including these regions might introduce. In addition, limitation to the area covered by the CO surveys enables a comparison with the results obtained in Paper II for the outer Galaxy, where the H_2 contribution was assumed to be negligible.

Unlike our approach in Paper II, here the areas in the second quadrant (and in the Carina region) that contain point-like gamma-ray sources (Swanenburg et al., 1981) were not taken out, because they were found to be close to CO concentrations that may account for the gamma-ray excesses. Pollock et al. (1985) have shown that a few of the first-quadrant point sources can result from CO concentrations. They have also shown that some point sources are present in addition to the gamma-ray estimates from CR-gas interactions in the first quadrant, and these point sources have been included in our model as described by Pollock et al. The influence of these known gamma-ray sources on the present large-scale analysis is negligible, because they contribute only a small fraction to the total gamma-ray flux; fits without the sources confirm this conclusion.

Given the limited counting statistics of the gamma-ray observations, it is not meaningful to start the correlation analysis with the large number of free parameters that has been introduced in Sect. 2.1. In most of the following analyses, therefore, we assume that the ratio $N(H_2)/W_{CO}$ is constant throughout the Galaxy, implying that $Y_{1j} = Y_{2j} = Y_{3j} = Y_{4j} \equiv Y_j$ ($j = 1, 2, 3$). Starting from a general case of six parameters for each energy range (q_{ij}, Y_j, I_{bj}; 18 in total) we tested whether various simpler models with fewer parameters give significantly worse fits to the data. In general, if a model has n free parameters we except $-2 \ln \lambda$ to have a chi-quare distribution with 18-n degrees of freedom, where λ is again the maximum-likehood ratio (now between the simpler model and the general one; Eadie et al., 1971). In principle, the number of free parameters in the general model is larger than 18 and in the simpler models larger than n, because the fluxes of the point sources have been made adjustable; since the calculation of the degrees of freedom remains unaffected (the same sources are included in all models), for the sake of clarity the extra free parameters have been omitted from the notation.

3. Results: the distribution of gamma-ray emissivities and $N(H_2)/W_{CO}$

3.1. *Fit results*

Using the likelihood procedure described above, the six parameters q_{ij} ($i = 1, 2, 3, 4$), Y_j, and $I_{b,j}$ were estimated for each energy interval j. Table 1 a presents the maximum-likelihood estimates and formal errors; the Y_j-values listed there are the same, within uncertainties. Figure 3 shows the likelihood-ratio distributions of Y_j. Figure 4 shows the q_{ij}-values as a function of R.

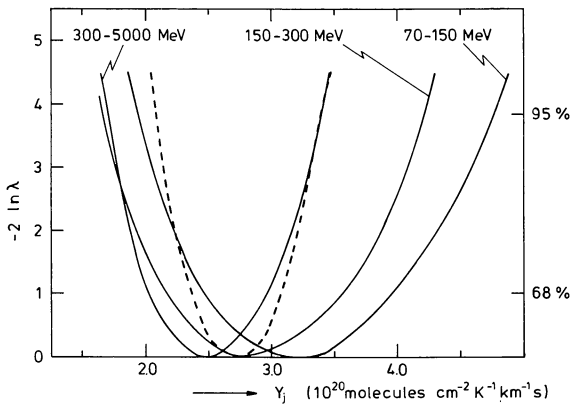

Fig. 3. Likelihood-ratio distribution of Y_j for each energy interval j (full lines). The dashed curve shows the likelihood-ratio distribution of the Y-parameter optimized over the three energy intervals together (Sect. 3.5)

Some fit parameters (and formal uncertainties) cannot be determined entirely independently, because the method encounters difficulties in distinguishing uniquely among some components. Although the angular distributions of the gas in the four distance intervals show distinct differences (Sect. 2), there are also large-scale similarities among some H I and CO maps, such as similar longitude coverage [e.g. $N(\mathrm{H\,I})_{3j}$ and $N(\mathrm{H\,I})_{4j}$] and concentration of all the gas in the galactic plane. These problematical similarities are most severe for analyses of the low-energy gamma rays, because the angular resolution of COS-B reduces with decreasing energy. Therefore, the radial emissivity distributions (Fig. 4) have to be judged carefully. An example of the effect of these similarities can be seen in Fig. 4 of Paper II, where the confidence regions (ellipses) of q_{3j} versus q_{4j} are presented; the axes of the ellipses are not parallel to the coordinate axes. The likelihood tests in the remainder of this section allow for such dependencies.

The emissivity values for $R > 10$ kpc agree with those in Paper II; by analysing nearly the entire second and third quadrants ($|b| < 10°$) in Paper II we were able to distinguish better between the contributions from the two distance ranges and to reduce significantly the statistical uncertainties, although small (5 %–10 %) systematic incertainties were introduced by neglecting H_2. The near constancy of the gamma-ray emissivity outside the solar circle for the 300 MeV–5 GeV range, deduced in Paper II, is consistent with the present findings. For each energy range the emissivity value in the 2–8 kpc range is higher than both that in the 8–10 kpc range and the values outside the solar circle. This trend seems to be energy dependent, being strongest for low energies, but has to be tested carefully, as stated above.

Figure 5 compares longitude profiles of the observed gamma-ray intensities with those estimated from the model that uses the fit parameters listed in Table 1a. The corresponding latitude profiles for selected longitude intervals are shown in Fig. 6. Although the fit parameters were determined in the range $-4°.5 < b < 6°.5$, the latitude profiles show a good agreement between the observed and the predicted gamma rays, even at higher latitudes. Since the predictions in these regions were derived almost entirely from only H I, the agreement indicates that the poor CO coverage at these latitudes has a negligible impact on our findings.

3.2. *Significance of the emissivity gradients*

To test the hypothesis of a constant gamma-ray emissivity throughout the Galaxy we repeated the fitting procedure for each individual energy range, this time forcing the emissivity values in the four distance intervals to be the same ($q_{1j}=q_{2j}=q_{3j}=q_{4j}$), while, again, Y_j and $I_{b,j}$ were free parameters. Within these constraints on the gamma-ray emissivities, we obtained $-2\ln\lambda = 72.8$. Given that this model has 9 free parameters, we expect that $-2\ln\lambda$ has a chi-square distribution with $18-9=9$ degrees of freedom (Sect. 2.4), so that $-2\ln\lambda = 72.8$ corresponds to a formally very low chance probability of $\sim 10^{-11}$. This result implies that the hypothesis of a constant gamma-ray emissivity as a function of R can be rejected for the integral 70 MeV–5 GeV energy range. Possible differences in the required emissivity gradients for each individual energy range will be studied in the following subsections.

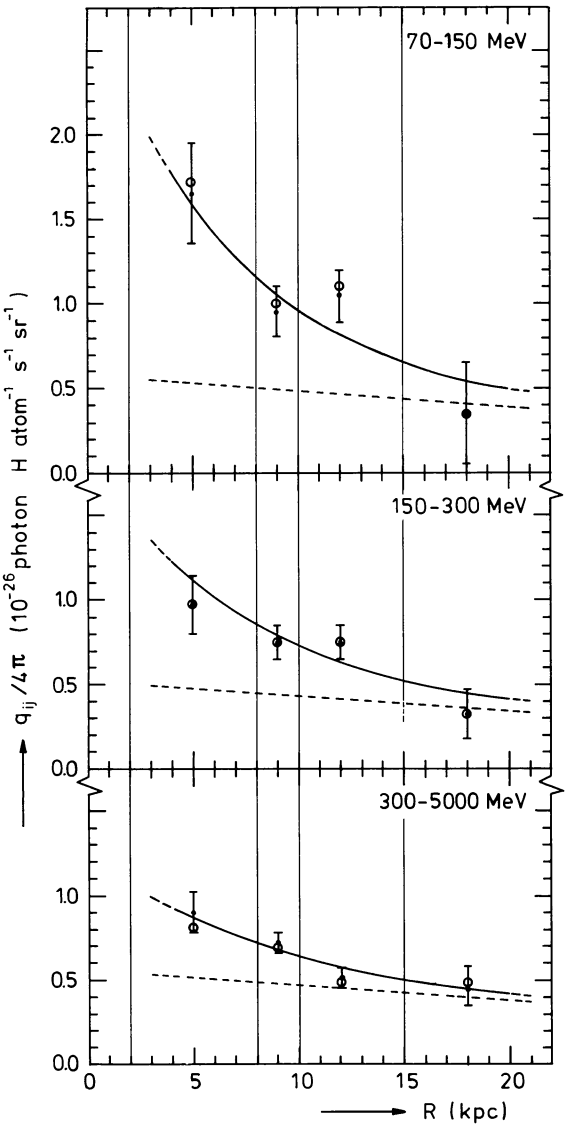

Fig. 4. Galacto-centric distribution of the gamma-ray emissivity for three energy intervals j. The black dots, together with formal 1σ error bars, indicate the fit values for selected distance ranges i (indicated by the vertical lines) without any constraints (Sect. 3.1; Table 1a). The circles are the emissivity values when the values of Y_j are forced to be identical (Sect. 3.5; Table 1c). The full curves represent the emissivity distributions $q_j(R)$ in the case of exponential distributions for the CR electrons and nuclei (Sect. 4.2). The dashed curves indicate the π^0-decay contribution from the CR nuclei, determined in Sect. 4.2 ($f=1$)

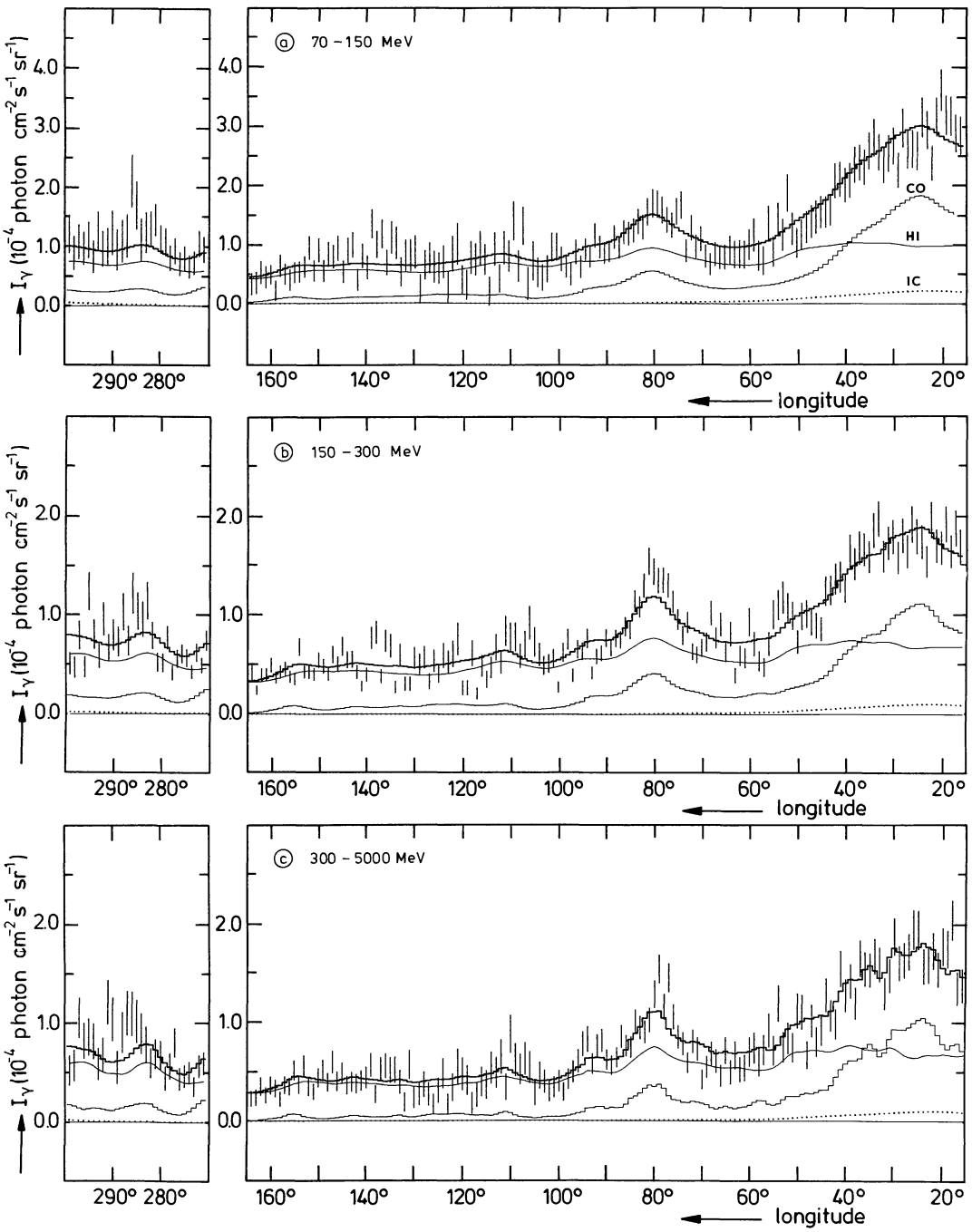

Fig. 5a–c. Longitude profiles ($-4°.5 < b < 6°.5$) of the observed gamma-ray intensities (bars; 1σ statistical uncertainties) and the estimates from CR interactions with the gas and photon fields for three energy ranges (**a–c**), using the fit parameters listed in Table 1 a. The thick lines represent the total estimates. The contributions from H I, CO, and inverse-Compton emission are indicated. The thin horizontal lines are the zero levels (the isotropic background level is subtracted from the observations). Point-like gamma-ray sources are not included in the predicted curves (e.g. in the Cygnus region around $l = 80°$ and in the Carina region around $l = 285°$)

3.3. Significance of the energy-dependent differences

The results presented in Sect. 3.1 suggest that Y_j is independent of energy and that the emissivity gradient is stronger for low energies than for high energies. Before studying the significance of each of these two effects we investigated whether the gamma-ray observations really *require* an energy-dependent model. We therefore considered the hypothesis of identical radial distributions of the gamma-ray emissivity q_{ij} for each energy interval j ($q_{11}:q_{21}:q_{31}:q_{41} = q_{12}:q_{22}:q_{32}:q_{42} = q_{13}:q_{23}:q_{33}:q_{43}$), together with identical Y_j-values ($Y_1 = Y_2 = Y_3$). Again, the background levels were free, making a total of 10 free parameters. It was found that $-2 \ln \lambda = 69.0$, which corresponds to a very low probability level (18 − 10 = 8 degrees of freedom) of $6\ 10^{-12}$, implying that the

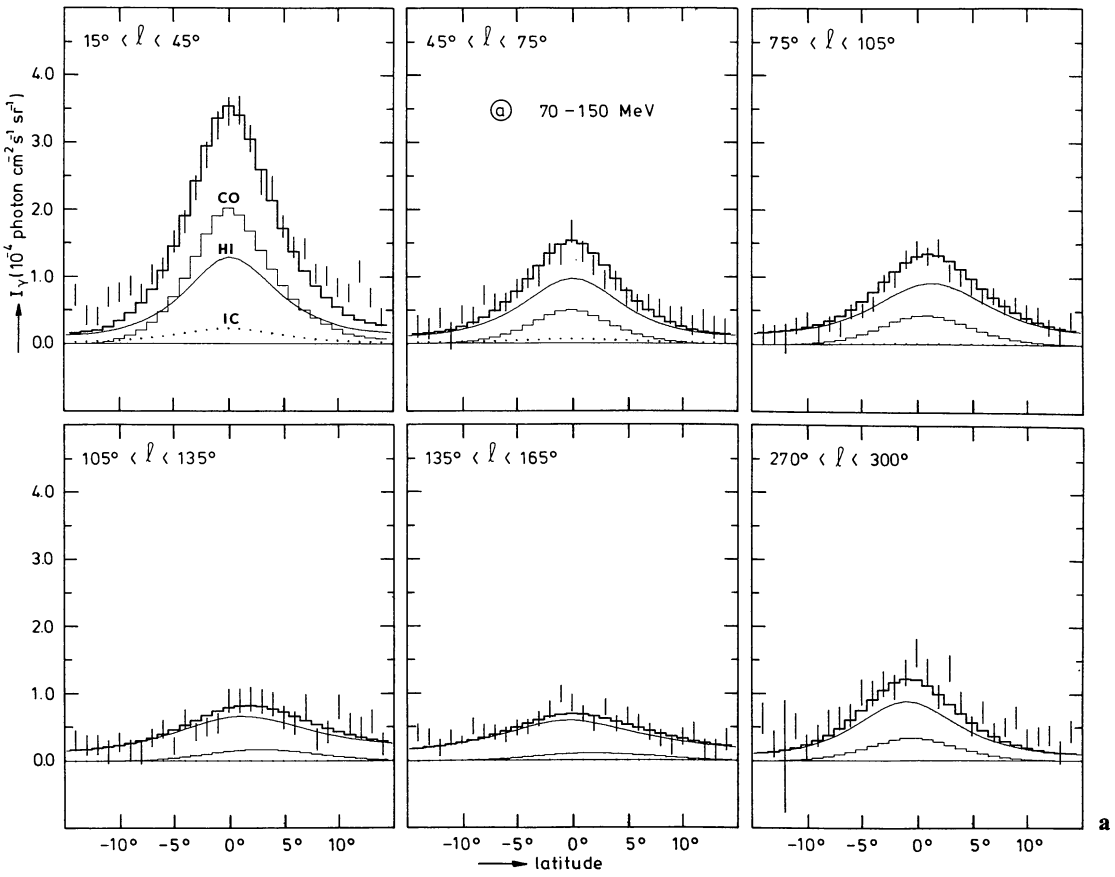

a

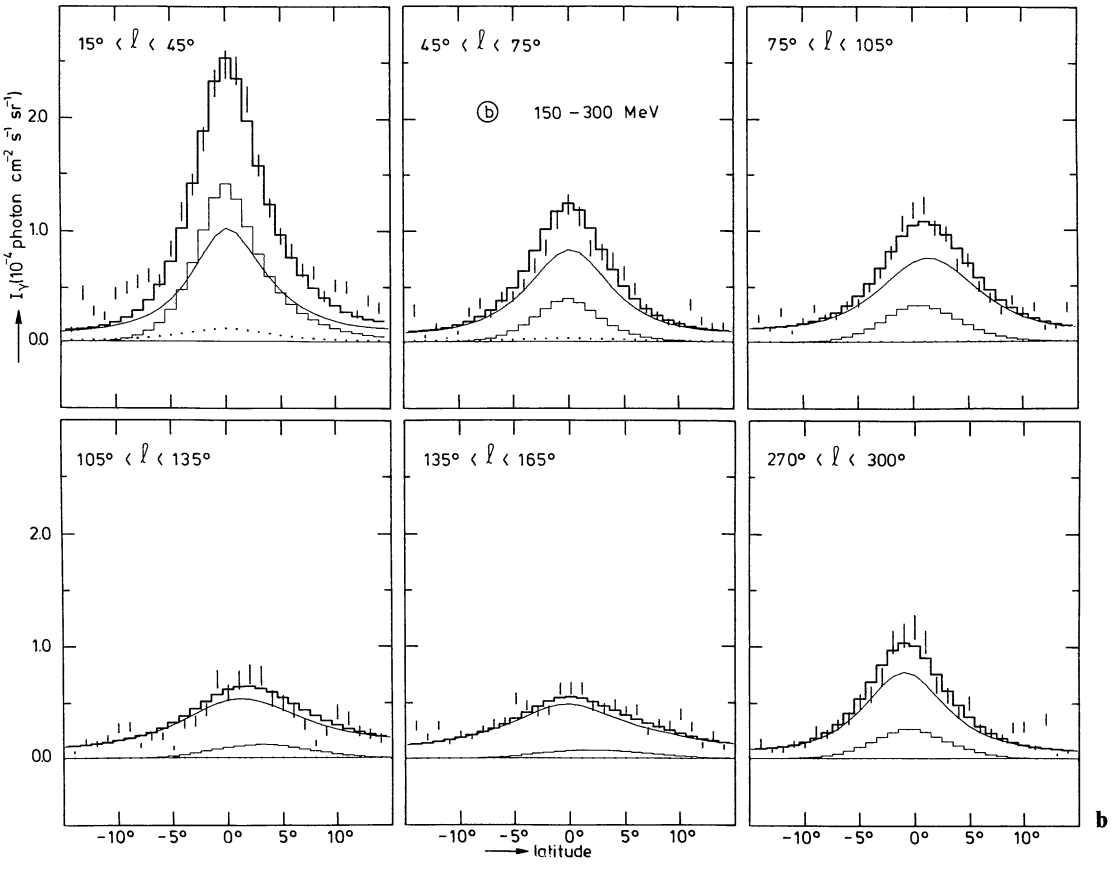

b

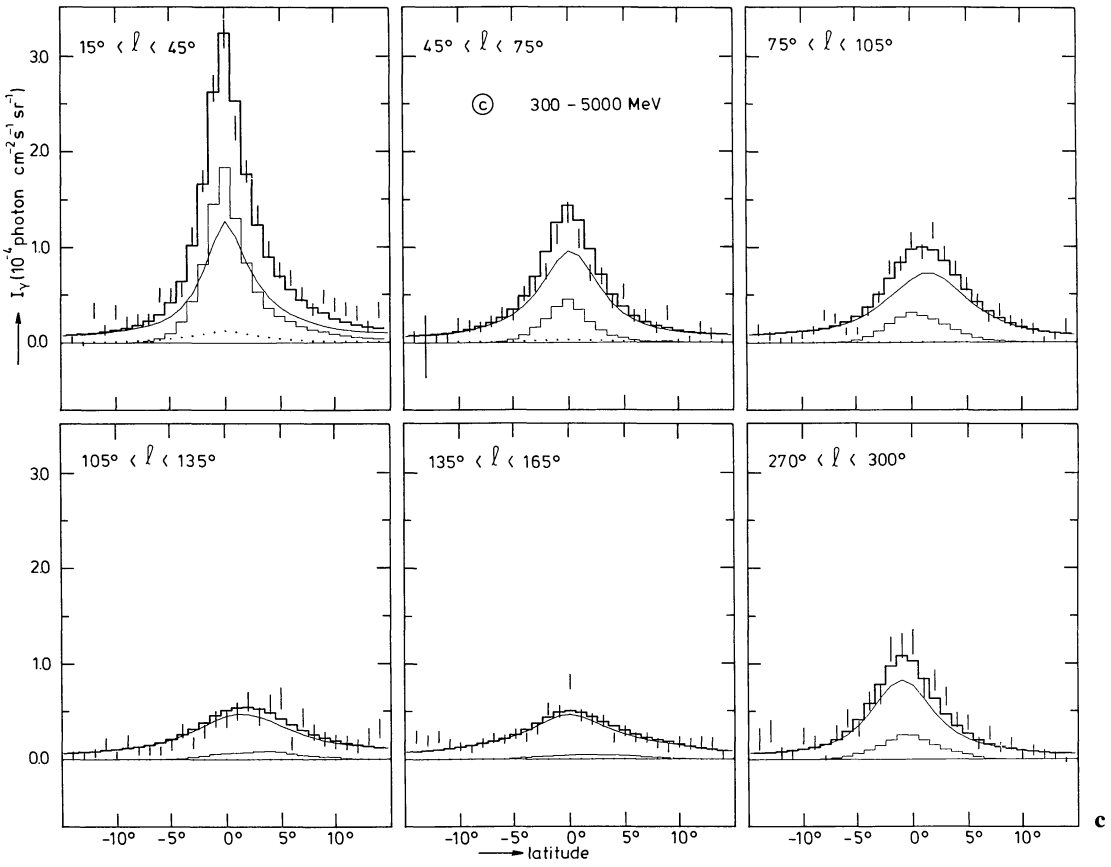

Fig. 6a–c. Latitude profiles of the observed gamma-ray intensities and the estimates from CR interactions with the gas and photon fields for three energy ranges (**a–c**), using the fit parameters listed in Table 1a which were determined for the latitude range $-4°.5 < b < 6°.5$. The meaning of the curves is the same as in Fig. 5. The isotropic background is subtracted from the observations

Table 1. Maximum-likelihood estimates of the six fit parameters for three energy ranges ($j=1, 2, 3$), determined from the comparison of $I_{\gamma,j}$ with $N(\mathrm{H\,I})$, W_{CO}, and the IC predictions in four distance intervals ($i=1, 2, 3, 4$ corresponds to $2\,\mathrm{kpc} < R < 8\,\mathrm{kpc}$, $8\,\mathrm{kpc} < R < 10\,\mathrm{kpc}$, $10\,\mathrm{kpc} < R < 15\,\mathrm{kpc}$, and $R > 15\,\mathrm{kpc}$, respectively). The area analyzed covers the first and second galactic quadrants and the Carina region. (a) Fit values for each individual energy range (Sect. 3.1). (b) Fit values when the emissivity gradient is forced to be the same for the three energy ranges (Sect. 3.4). (c) Fit values when the values of Y_j are forced to be identical (Sect. 3.5)

Energy range	10^{-26} ph H at^{-1} s^{-1} sr^{-1}				10^{20} mol · cm^{-2} K^{-1} km^{-1} s	10^{-5} ph cm^{-2} s^{-1} sr^{-1}	
MeV	$q_{1j}/4\pi$	$q_{2j}/4\pi$	$q_{3j}/4\pi$	$q_{4j}/4\pi$	Y_j	$I_{b,j}$	
70– 150	1.65±0.3	0.95±0.15	1.05±0.15	0.35±0.3	3.2±0.7	4.7±0.8	
150– 300	0.97±0.17	0.74±0.09	0.74±0.10	0.32±0.15	2.8±0.7	2.0±0.4	(a)
300–5000	0.90±0.12	0.72±0.06	0.51±0.06	0.46±0.12	2.5±0.5	2.4±0.3	
70– 150	1.25	0.95	0.95	0.52	4.1	4.5	
150– 300	0.97	0.73	0.73	0.41	2.8	2.0	(b)
300–5000	0.84	0.63	0.63	0.35	2.8	2.2	
70– 150	1.80	1.02	1.13	0.35		4.5	
150– 300	0.98	0.75	0.75	0.32	2.75±0.35	2.0	(c)
300–5000	0.83	0.68	0.49	0.48		2.4	

gamma-ray observations require an interpretation with Y_j energy dependent (Sect. 3.4), or with energy-dependent emissivity gradients (Sect. 3.5), or both.

The need of such an energy-dependent model is not surprising: Mayer-Hasselwander (1983), comparing the gamma-ray sky maps for low and high energies, showed the presence of a systematic variation of the spectral ratio – the ratio between the intensities for low and high energies – along the galactic plane, and, more specifically, that the spectrum towards the inner part of the Galaxy is softer than that of the remainder of the disk.

3.4. *Different emissivity spectra for* H I *and* H_2 *?*

We investigated whether the spectral difference found above can be ascribed solely to different shapes of the emissivity spectra for the H I and H_2 contributions(i.e. different Y_j-values). This hypothesis again requires forcing the ratios between the emissivity values in the four distance intervals to be the same for the three energy ranges, so this model has 12 free parameters. The resultant maximum-likelihood estimates of the fit parameters are given in Table 1b. It was found that $-2\ln\lambda = 19.9$, a value that corresponds to a chance probability ($18-12=6$ degrees of freedom) of $3\ 10^{-3}$. It can be concluded that this hypothesis, which adopts identical emissivity gradients and attributes all the energy dependence (Sect. 3.3) entirely to different emissivity spectra for the H I and H_2 contributions, is less satisfactory than the general 18-parameter model.

3.5. *Energy-dependent emissivity gradients?*

The second possibility that might account for the energy dependence concerns different radial distributions of the gamma-ray emissivities. We therefore evaluated the hypothesis that all the energy dependence of the model is due to different emissivity gradients and that the Y_j-values are identical ($Y_1 = Y_2 = Y_3 \equiv Y$). The resultant maximum-likelihood estimates are given in Table 1c and the emissivity values are indicated in Fig. 4. The likelihood-ratio distribution of Y is included in Fig. 3. The model has 16 free parameters, and it was found that $-2\ln\lambda = 1.4$. In this model, $-2\ln\lambda$ has a chi-square distribution with $18-16=2$ degrees of freedom, which implies a reduction of the likelihood within the 1σ level. This hypothesis of the energy-independence of Y_j, which implies an energy-dependent emissivity gradient, is therefore as good as the general 18-parameter model.

3.6. *Variations of* $N(H_2)/W_{CO}$ *throughout the Galaxy?*

Until now we have assumed that the ratio $X = N(H_2)/W_{CO}$ is constant throughout the Galaxy ($Y_j = Y_{1j} = Y_{2j} = Y_{3j} = Y_{4j}$). To investigate possible large-scale variations of X throughout the Galaxy, the Y-values were determined separately for the intervals $2\,\text{kpc} < R < 8\,\text{kpc}$ ($Y_j(2\text{–}8\,\text{kpc}) \equiv Y_{1j}$) and $R > 8\,\text{kpc}$ ($Y_j(>8\,\text{kpc}) \equiv Y_{2j} = Y_{3j} = Y_{4j}$). Because of the relatively wide point-spread functions of COS-B for the 70–150 MeV and 150–300 MeV ranges, the introduction of an additional free parameter into the fits for these two energy intervals did not turn out to be meaningful, so the analysis was restricted to the high-energy range and the integral range (70 MeV–5 GeV). In the latter case, the emissivity values were optimized for each energy range separately. The resultant confidence region of Y in both distance intervals (Fig. 7) indicates that the Y-values are identical within uncertainties. The maximum-likelihood estimates for the 70 MeV–5 GeV range are: $Y(2\text{–}8\,\text{kpc}) = (2.8\pm0.7)\ 10^{20}\,\text{mol}\cdot\text{cm}^{-2}\,\text{K}^{-1}\,\text{km}^{-1}\,\text{s}$, $Y(>8\,\text{kpc}) = (2.7\pm0.4)\ 10^{20}\,\text{mol}\cdot\text{cm}^{-2}\,\text{K}^{-1}\,\text{km}^{-1}\,\text{s}$, and $Y(2\text{–}8\,\text{kpc})/Y(>8\,\text{kpc}) = 1.0\pm0.3$.

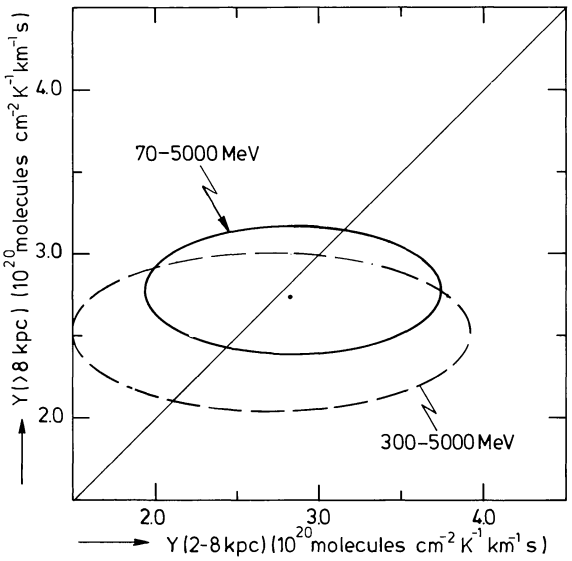

Fig. 7. Confidence region of $Y(2\text{–}8\,\text{kpc})$ and $Y(>8\,\text{kpc})$, related to the ratio $N(H_2)/W_{CO}$ in the two distance intervals, for the 300 MeV–5 GeV energy range (dashed curve) and for the integral energy range (70 MeV–5 GeV; full curve) as determined in Sect. 3.6. The 68 % confidence levels were determined from the distribution of the likelihood ratio λ and correspond to $-2\ln\lambda = 2.4$ (chi-square distribution with 2 degrees of freedom)

The implication of this result and of the good quality of the fit (see Figs. 5 and 6) is that, within the limitations and uncertainties of our analysis, CO is an acceptable large-scale tracer of H_2 mass. The uncertainties and wide distance intervals, however, permit small-scale CO/H_2 variations within the Galaxy, a point discussed in Sect. 5.2.

4. Results: the distribution of cosmic-ray electrons and nuclei

4.1. *General considerations*

On the assumption that CR interactions with the gas and photon fields are responsible for the observed gamma-ray emission, knowledge of the radial distribution of gamma-ray emissivities enables the determination of the radial distribution of cosmic rays in the Galaxy. In addition, the energy dependence can be used to study separately the distribution of CR electrons and nuclei. We assume that the shapes of the CR spectra do not strongly vary throughout the Galaxy and that the scale height of the cosmic rays is significantly larger than that of the gas. The derived CR gradients are upper limits if a population of unresolved galactic gamma-ray sources exists with a latitude distribution similar to that of the gas but with a stronger concentration towards the inner part of the Galaxy.

The emissivity distributions found in the preceding section permit some qualitative conclusions. The radial distribution of the gamma-ray emissivity for the 300 MeV–5 GeV range indicates that the density of CR nuclei of a few GeV (those responsible for the

bulk of the gamma-ray emission in the 300 MeV–5 GeV range by the π^0-decay process) can be only weakly dependent on R. For instance, in the case of a linear decrease, the gradient cannot be stronger than about -6%/kpc relative to the local ($R=10$ kpc) density of CR nuclei. In particular, outside the solar circle the emissivity (and thus also the CR nuclei density) shows no strong decrease, a finding consistent with the near constancy found in Paper II from a more extended analysis of the outer Galaxy alone. By contrast, the overall decrease of the gamma-ray emissivity for the 70–150 MeV range, which is stronger than for high energies (see preceding section), indicates a large-scale galacto-centric gradient for electrons with energies below ~ 300 MeV (those responsible for a large fraction of the gamma-ray emission in the 70–150 MeV range by the bremsstrahlung process). The CR nuclei contribute significantly (probably about 50%; see Sect. 4.2) to the local emissivity for the 70–150 MeV range. The very small gradient of the nuclei therefore implies that, with a linear decrease as a function of R, the gradient of the CR electron density is probably as large as roughly -30%/kpc relative to the local density. If a population of unresolved steep-spectrum gamma-ray point sources is present in the inner Galaxy, evidently a less steep CR electron gradient would be required.

4.2. *Exponential distributions*

For a more quantitative statement about the galactic distribution of CR particles, one has to know the π^0-decay contribution from the CR nuclei $q_{n,j}(R_\odot)$ and the bremsstrahlung contribution from the CR electrons $q_{e,j}(R_\odot)$ to the total local gamma-ray emissivity $q_j(R_\odot)$ for each energy interval $j=1$, 2, 3 ($q_j(R)=q_{e,j}(R)+q_{n,j}(R)$). The total gamma-ray emissivity at galacto-centric distance R can be represented by

$$q_j(R)=\frac{n_e(R)}{n_e(R_\odot)}\cdot q_{e,j}(R_\odot)+\frac{n_n(R)}{n_n(R_\odot)}\cdot q_{n,j}(R_\odot), \tag{3}$$

where $n_e(R)$ and $n_n(R)$ are the densities of CR electrons and nuclei, respectively. The spectral shape of the π^0-decay contribution to the local gamma-ray emissivities was estimated from the work of Stephens and Badhwar (1981) based on the demodulated local proton spectrum: $q_{\pi^0,j}/4\pi=(0.48\pm 0.04)\ 10^{-26}$, $(0.43\pm 0.06)\ 10^{-26}$, $(0.47\pm 0.02)\ 10^{-26}$ photon H atom^{-1}s^{-1} sr^{-1} for the 70–150 MeV, 150–300 MeV, and 300 MeV–5 GeV energy ranges, respectively. The small uncertainties in these numbers (representing the uncertainties in the demodulation of the proton spectra used by Stephens and Badhwar) make this a reasonable approach. The demodulated proton flux measured near the earth may not be typical for the local interstellar medium. We therefore adopted $q_{n,j}(R_\odot)=f\cdot q_{\pi^0,j}$, where f is an energy-independent scaling factor, and considered a range of possible f values. Assuming exponential CR distributions, the total gamma-ray emissivity can be written as:

$$q_j(R)=e^{S_e(R-R_\odot)}\cdot[q_j(R_\odot)-f\cdot q_{\pi^0,j}]+e^{S_n(R-R_\odot)}f\cdot q_{\pi^0,j}. \tag{4}$$

In principle, with Eq. (4) the gamma-ray emissivities for the four distance intervals (Table 1a; Fig. 4) can be fitted by a least-squares method to obtain coarse estimates of the five parameters S_e, S_n, and $q_j(R_\odot)$ ($j=1,2,3$). However, a least-squares method can be applied strictly only if the measurements (here emissivity values), and the corresponding formal uncertainties as well, are independent; this is not the case (Sect. 3.1). The best approach is again to use the likelihood method (which allows for these dependencies), with q_{ij} in Eq. (1) replaced by the expression in Eq. (4), and to estimate the five new parameters instead of the 12 emissivities q_{ij} (with Y_j and $I_{b,j}$ a total of 11 parameters). We used a simplified approach because of the weak dependency between the derived emissivities inside and outside the solar circle, due to the different regions of the sky that dominate in the determination of the emissivities: the first galactic quadrant evidently dominates in the determination of the emissivities for the inner Galaxy, while the second quadrant dominates in the determination for the outer Galaxy. The two emissivity values outside the solar circle, and the two emissivity values inside the solar circle as well, are to some extent related. Using only the likelihood distribution of q_{1j} versus q_{2j} and of q_{3j} versus q_{4j} is therefore sufficient (Sect. 3.1; $3\times 2=6$ confidence regions in all). The values of the five parameters were estimated by maximizing the likelihood over the three energy ranges.

Table 2 presents the values of S_e and S_n for $f=0.8$, 1.0, and 1.2. If we force $S_e=S_n\equiv S$ (although this equality is in fact not acceptable, as the tests in Sect. 3 and the results presented in Table 2 indicate), then $S=-0.07\pm 0.02$ kpc^{-1}, independent of f. The maximum-likelihood estimates of the total local gamma-ray emissivities $q_j(R_\odot)/4\pi$ were found to be independent of the f value chosen: $(0.96\pm 0.08)\ 10^{-26}$, $(0.72\pm 0.05)\ 10^{-26}$, and $(0.63\pm 0.04)\ 10^{-26}$ photon H atom^{-1}s^{-1}sr^{-1}, for the 70–150 MeV, 150–300 MeV, and 300 MeV–5 GeV ranges, respectively (for a comparison with previous estimates of the local gamma-ray emissivity see Sect. 5.4).

The range of possible f values is limited to $0.8\leqq f\leqq 1.2$ for the following reasons: (1) A value of f less than 0.8 is unlikely, because it would imply that $S_n>0$ (see Table 2), i.e., an increase of the CR nuclei density with R; (2) A value of f larger than ~ 1.2 results in a steep bremsstrahlung spectrum ($q_{e,j}=q_j-f\cdot q_{\pi^0,j}$), which implies a too step electron spectrum $I_e(q_e(E_\gamma)\propto \frac{1}{E_\gamma}\int_{E_\gamma}^{\infty} I_e(E_e)\,dE_e)$, for $E_e\gtrsim 300$ MeV (up to several GeV) compared with the electron spectrum derived from low-frequency radio observations of the anti centre and polar directions (Rockstroh and Webber, 1978; Webber et al., 1980; Webber, 1983). The latter seems to be well established. This radio spectrum corresponds to an electron spectral index of $\alpha=2.3$ at $E_e\simeq 1$ GeV ($I_e\propto E_e^{-\alpha}$), but $f>1.2$ requires $\alpha\gtrsim 2.6$ for $E_e\gtrsim 300$ MeV. For a discussion of the electron spectrum see Sect. 5.4.

For all f values, $-2\ln\lambda$ is in the range 10.1 to 11.3, corresponding to a chance probability ($18-11=7$ degrees of freedom) of $\sim 15\%$, that implies that this simplified model with exponential CR distributions gives an almost equally acceptable description of the gamma-ray observations compared to the general model with 12 emissivities. The resultant radial distributions of the gamma-ray emissivities, as defined in Eq. (4) ($f=1.0$), are included in Fig. 4.

Table 2. Values of the parameters S_e and S_n, which describe the exponential radial density distributions of CR electrons and nuclei, for different f values (see Sect. 4.2)

f	S_e (kpc^{-1})	S_n (kpc^{-1})
1.2	$-0.18+0.04$ -0.03	$-0.04+0.015$ -0.015
1.0	$-0.16+0.05$ -0.03	$-0.02+0.015$ -0.03
0.8	$-0.14+0.05$ -0.03	$0.00+0.015$ -0.05

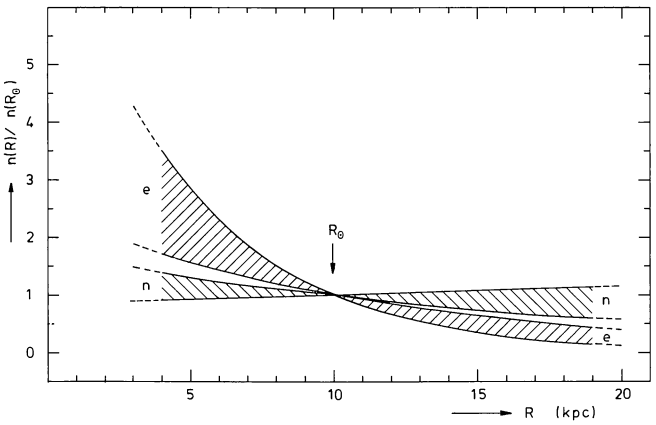

Fig. 8. Radial CR-density distributions (relative to the local density at $R_\odot = 10$ kpc) of the form $e^{S(R-R_\odot)}$, for CR electrons (e) and nuclei (n), as determined in Sect. 4.2. The hatched areas encompass $0.8 \leqq f \leqq 1.2$ (Sect. 4.2) and 1σ uncertainties for S_n and S_e, that is in all $-0.21 < S_e < -0.09$ and $-0.055 < S_n < +0.015$. Note that within these hatched areas S_e and S_n are not independent: a stronger electron gradient implies a stronger gradient for the nuclei (see Table 2)

The main conclusions from this analysis are that (1) if we force $S_e = S_n$, we find only a weak gradient in the CR density distribution throughout the galactic plane (corresponding to a radial scale length of 15 ± 4 kpc), (2) the gradient in the CR electron component is required by the data (Table 2), whereas (3) the data are consistent with a constant CR nuclei density throughout the entire galactic plane. Figure 8 presents the CR distributions that result from our analysis (Table 2); the hatched areas encompass $0.8 \leqq f \leqq 1.2$ and 1σ uncertainties for S_n and S_e. The corresponding scale lengths are 4–11 kpc for CR electrons and >18 kpc for CR nuclei.

5. Discussion

5.1. Systematic uncertainties

Our detailed statistical analysis would not be meaningful if there were large systematic uncertainties. The influence of possible unresolved gamma-ray point sources on the value of X and on the emissivity and CR distributions has been mentioned in previous sections and, where appropriate, will be discussed in the following ones, but in this section we concentrate on the systematic uncertainties in the observations and in the treatment of the data.

The radial distribution of the gamma-ray emissivities depends only weakly on the rotation curve used, owing to the wide distance intervals chosen. The use of a somewhat different rotation curve and different $R_\odot$ value would have changed basically only the absolute distance scale of the radial gas distribution and, thus, of the radial distribution of the gamma-ray emissivities found (see Paper II). The radial scale lengths of the cosmic rays determined in Sect. 4.2 should be scaled accordingly. The value of X is not affected.

The systematic uncertainties in the COS-B gamma-ray data are small compared with the statistical uncertainties. A decline of instrumental sensitivity with time in orbit was corrected by comparing the measured intensities of selected regions along the galactic plane at different epochs (Strong et al., 1985a, c). Similarly, the smooth decrease of instrumental background with time (Mayer-Hasselwander et al., 1982) was taken into account. The uncertainties in these corrections introduce systematic uncertainties of 10% or less in the gamma-ray data. In addition, these uncertainties are not expected to be correlated with one of the components of our model. The absolute background levels for the three energy ranges were free parameters in our analysis and introduce therefore no additional systematic error; the levels were found to be consistent with other recent studies of the COS-B data. Our gamma-ray intensity distributions are in satisfactory agreement with the gamma-ray observations by the SAS-2 satellite; the outer-Galaxy data of SAS-2 were analysed in Paper II and the results were found to be in agreement with the COS-B findings. X is not influenced by systematic uncertainties in the calibration of the absolute gamma-ray intensities.

To check the effects of possible differences in calibration between the northern- and southern- hemisphere radio surveys, the analysis was repeated for only the first and second quadrants (Carina excluded). The results were found to be the same within statistical uncertainties. The noise in the CO and H I observations is unimportant in our work, owing to the convolution with the COS-B point-spread function. Calibration errors in the CO data, probably 10%–20%, affect the X value by this same factor (see Sect. 5.2); the emissivity distributions are not affected. The systematic errors in the H I data ($\sim 10\%$) are small compared with the statistical uncertainties in this work and, in any event, introduce only an absolute scaling factor for all q_{ij} values; the radial dependence of the emissivity values remains unaffected. The optical-depth corrections for H I, however, are poorly understood and, in principle, might give systematic effects. We made a first-order optical-depth correction, assuming a uniform spin temperature of 125 K, but we found that adopting other temperatures that differ by values up to ± 15 K (an acceptable range for large-scale analyses) changes N(H I) generally by less than 4%. Differences up to 10% were found for the mid plane ($|b| < 0.^\circ 5$) in the first quadrant ($10^\circ \lesssim l \lesssim 70^\circ$); only in small regions with the strongest velocity crowding ($70^\circ \lesssim l \lesssim 80^\circ$ and $280^\circ \lesssim l \lesssim 290^\circ$; $|b| \lesssim 3^\circ$) are differences up to 20% present. The uncertainties in the H I optical-depth corrections have therefore probably a marginal impact on our results. The major impact is probably for the gamma-ray emissivities in the 2–8 kpc range; if we underestimated the optical depths in the inner Galaxy, the radial distribution of the CR density becomes even flatter. The H I optical-depth effects do not affect the required energy-dependence of the model.

Last, the modelled IC contribution to the observed gamma-ray intensities for the three energy ranges is less than 5% for the entire sky area included in our analysis (Bloemen, 1985), and the uncertainties in the IC intensities therefore marginally influence our findings; even neglecting the IC emission or increasing it by a factor of two has no significant impact on our conclusions.

5.2. Gamma rays from molecular hydrogen and $N(H_2)/W_{CO}$

The ratio $N(H_2)/W_{CO}$ is frequently used to determine the distribution of H_2 in the Galaxy from CO surveys. The $J=1-0$ transition of CO is optically thick in large molecular clouds, so that it is not evident that this transition can be used to obtain H_2 column densities. Differential galactic rotation partly alleviates the problem by Doppler shifting clouds at different galactic radii, so that shadowing of distant clouds by nearer clouds is unimportant. $N(H_2)/W_{CO}$ is probably not constant for individual clouds, but when averaged over a large number of clouds on a galactic scale it appears to be useful to estimate the mass of H_2. The determination

and application of the quantity $N(H_2)/W_{CO}$ have been controversial, in part because galactic temperature and abundance gradients can have a significant effect on the conversion. In this section we discuss a way of determining $N(H_2)/W_{CO}$, using the COS-B gamma-ray data, that circumvents the previous difficulties.

The hypothesis of identical Y_j values, which was found fully acceptable (Sect. 3.5), implies [following Eq. (2)] that the spectral shapes of the gamma rays from H I and H_2 are the same. Because the cosmic rays responsible for the production of low-energy gamma rays have generally lower energies than those responsible for the production of high-energy gamma rays, it can be concluded that we find no significant indication of energy dependence in the CR penetration of molecular clouds. In fact, the theoretical work of Skilling and Strong (1976) and Cesarsky and Völk (1978) indicates that only very low-energy protons and electrons (<50 MeV) fail to penetrate a dense cloud completely. Furthermore, the gamma-ray observations of the Orion molecular complex show conclusively that cosmic rays do penetrate at least the local giant molecular clouds (Bloemen et al., 1984a). If the average CR density inside the molecular clouds is indeed the same as in the atomic-hydrogen gas, then, following Eq. (2), the Y-parameter represents X, best estimated as $X=(2.75\pm0.35)\,10^{20}$ mol $\cdot$ cm^{-2}K^{-1}km^{-1}s (Sect. 3.5). As mentioned before, however, if a population of unresolved galactic gamma-ray point sources distributed like CO exists, Y would be an overestimate of X (see also Lebrun et al., 1983). Taking into account all systematic uncertainties mentioned in Sect. 5.1 a more realistic estimate of the true uncertainty of X is probably a factor of ~2 times the formal error. This value of X is unaffected by the presence of helium as long as the relative abundance of helium is, as expected, the same in the atomic and molecular clouds.

The X value derive is independent of excitation, abundance, and optical-depth effects, which have plagued previous determinations. It is also free of assumptions of virial equilibrium of molecular clouds, known to be violated in the high-latitude CO clouds surveyed by Magnani et al. (1985). Our X value represents a global average over the entire Galaxy, and is, we believe, the best value to use for estimating the H_2 content of the Galaxy from CO surveys. We note, however: (1) Our value should strictly be regarded as an upper limit (because of a possible point-source contribution). (2) Our value was determined using the Columbia/GISS CO survey; systematic differences between the Columbia/GISS data and other surveys would change this value proportionally if these data had been used. (3) We showed (in Sect. 3.6) that X is constant on a few-kpc scale throughout the Galaxy; since small-scale variations in X cannot be excluded, the use of our conversion at a resolution finer than the one used to determine X, should take this possibility of variations into account. The gamma-ray observations do not provide a stringent lower limit on X. The good correlation between the observed gamma-ray intensities and the estimates from the gas and the agreement between our X value and the X value derived by Bloemen et al. (1984a) from a similar analysis of the Orion region (where the source contribution is probably negligible), however, suggests that

Table 3. Principal determinations of $N(H_2)/W_{CO}$

Source	Quantity determined	Derived $N(H_2)/W_{CO}$	Calibration difference [a]
	mol $\cdot$ cm^{-2}	K^{-1}km^{-1}s	
Gordon and Burton (1976)	$N(H_2)/W_{CO}$	$2.3\ 10^{20}$	1.66 [c]
Dickman (1978)	$N(H_2)/N(^{13}CO)$	$1.5\ 10^{20}$	
Solomon and Sanders (1980)	$N(H_2)/W_{CO}$	$6.0\ 10^{20}$	1.27 [d]
Frerking et al. (1982)	$N(H_2)/W_{CO}$	$1.8\ 10^{20}$ [g]	
Lebrun et al. (1983) [b]	$N(H_2)/W_{CO}$	$1–3\ 10^{20}$	
Black and Willner (1984)	$N(H_2)/N(CO)$	$<3\ 10^{20}$	
Bloemen et al. (1984) [b]	$N(H_2)/W_{CO}$	$2.6\ 10^{20}$	
Lebrun and Huang (1984)	$N(H_2)/W_{CO}$	$1.1\ 10^{20}$	
Sanders et al. (1984)	$N(H_2)/W_{CO}$	$3.6\ 10^{20}$	1.27 [d]
Bhat et al. (1985) [b]	$N(H_2)/W_{CO}$	$1.4\ 10^{20}$ [e]	
		$0.7\ 10^{20}$ [f]	
Dickman (1985)	$N(H_2)/N(^{13}CO)$	$2.2\ 10^{20}$	
This work	$N(H_2)/W_{CO}$	$2.8\ 10^{20}$	

[a] This is the ratio between the CO intensities of the surveys used by the authors listed in the first column and those of the Columbia/GISS survey used in the present work, as derived by Cohen et al. (1985b) (see Sect. 5.2)

[b] Using gamma-ray observations

[c] Data are similar to those used by Burton and Gordon (1978), which have been studied by Cohen et al. (1985b)

[d] Sanders et al. (1984) contained data both from the NRAO 11 m and the FCRAO 14 m telescopes; the NRAO data are the same as in Solomon and Sanders (1980), and the FCRAO data were scaled to agree with the NRAO calibration (Sanders 1985, private communication)

[e] Local

[f] At $R=6$ kpc

[g] Determined in the ϱ Oph region and recommended for galactic-survey work (no correlation between $N(H_2)$ and W_{CO} was found in the Taurus clouds)

Table 4a. Mass of H I and H_2 in the Milky Way

R (kpc)	σ_{H_2}/σ_{HI}	M(H I)[a] ($M_\odot$)	$M(H_2)$	R (kpc)	M(H I) ($M_\odot$)	$M(H_2)$
<0.5	–	2.3 10^6	<2 10^7 [b]	< 0.5	2.3 10^6	<2 10^7 [b]
2– 8	1.35	5.5 10^8	7.4 10^8	< 8	5.9 10^8	8.1 10^8
8–10	0.40	3.3 10^8	1.3 10^8	<10	9.2 10^8	9.4 10^8
10–15	0.20	1.1 10^9	2.3 10^8	<15	2.1 10^9	1.2 10^9

[a] Based on constant value of $\sigma_{HI} = 2.9\, M_\odot\, pc^{-2}$ (see text)
[b] Blitz et al. (1985), 1 σ upper limit

Table 4b. Other determinations of $M(H_2)$ (2–10 kpc) and corresponding ratio between H_2 and H I mass (2–10 kpc)

Source	$M(H_2)$ ($M_\odot$)	$M(H_2)/M$(H I)[a]
Scoville and Solomon (1975)	1–3 10^9	1–3
Gordon and Burton (1976)	2.1 10^9	2.4
Solomon and Sanders (1980)	4 10^9	4.5
Blitz and Shu (1980)	1 10^9 [b]	1.1
Liszt et al. (1981)	2.3 10^9	2.6
Dame (1983)	0.7 10^9	0.8
Lebrun et al. (1983)	0.9 10^9 [b]	1.0
Sanders et al. (1984)	2.6 10^9	3.0
Bhat et al. (1985)	0.6 10^9	0.7
This work	0.9 10^9	1.0

[a] M(H I) is taken to be 0.9 $10^9\, M_\odot$ (Henderson et al., 1982)
[b] This mass is derived from quantities given in the paper

the point-source contribution is not dominant in the gamma-ray component we have attributed to H_2. We therefore believe that X is not smaller than $\sim 1.5\ 10^{20}$ mol · cm^{-2} K^{-1} km^{-1} s.

We review the principal previous determinations of X in Table 3 (column 3). Some authors have determined the rare isotopic ratio $N(H_2)/N(^{13}CO)$ in the vicinity of the Sun. We converted their measured values to $N(H_2)/W_{CO}$, using standard assumptions (e.g. Solomon and Sanders, 1980). Column 4 gives the known calibration differences between the various surveys (Cohen et al., 1985b). These differences have to be considered when our H_2-mass estimates are compared to those of the other authors (Sect. 5.3).

Dickman (1985, private communication), has rederived the ratio $N(H_2)/N(^{13}CO)$ to much higher extinctions, showing that a linear relation exists to $A_v \simeq 20$ mag; we quote a value of $N(H_2)/W_{CO}$ derived from his new work. Since our value of X is a reliable upper limit, it favours the low value first advocated by Dickman (1978) and subsequently used by Blitz and Shu (1980) and others, rather than the value of Solomon and Sanders (1980).

On the other hand, the rough agreement between our X value and the other (low) values indicates that the contribution from a possible population of unresolved gamma-ray sources distributed like CO is probably small.

5.3. *The mass of H_2 in the Milky Way*

We can now use our X value to determine the H_2 mass of the molecular gas in the radial bins we used. The results are summarized in Table 4a (no helium correction is applied). First, the ratio between the H_2 and H I surface densities σ_{H_2}/σ_{HI} was calculated by direct integration of the maps presented in Figs. 1 and 2; σ_{H_2}/σ_{HI} is derived from the ratio between these integrals. Second, the H I masses were determined; σ_{HI} was assumed to be constant from $R = 2$ kpc to $R = 15$ kpc, as shown by Gordon and Burton (1976) and Blitz et al. (1983), and its value was derived from the total H I mass at $R < 10$ kpc of 9.2 $10^8\, M_\odot$ found by Henderson et al. (1982). The H_2 masses, then, follow from the values of the ratio σ_{H_2}/σ_{HI}. We estimate that our H_2 masses have uncertainties of 20 %–30 %. The H_2 mass for $R < 500$ pc was taken from the gamma-ray study by Blitz et al. (1985).

Most CO observers determine first the emissivity of CO vs. R, multiply by X, and then estimate H_2 masses by integration over the Galaxy. Dame (1983) applied this method to the Columbia CO data; scaling his H_2 masses with the ratio between our X value and the value he applied gives the same result.

Our results in Table 4a confirm the results first found by Scoville and Solomon (1975), Gordon and Burton (1976), and Cohen and Thaddeus (1977): the radial distributions of H I and H_2 (based on CO observations) are intrinsically different. Our contribution is that excitation and abundance effects in the CO do not alter this conclusion. Whereas previous authors have assumed a constant $N(H_2)/W_{CO}$, in this work the distribution of H_2 is inferred directly from the CO and the gamma-ray distributions.

We differ with several previous studies in the molecular fraction of the interstellar gas. Table 4b presents previous estimates of the mass of molecular hydrogen inside the solar circle. Our results are clearly inconsistent with the determinations of Gordon and Burton (1976), Solomon and Sanders (1980), Liszt et al. (1981), and Sanders et al. (1984). These inconsistencies can partly be explained by calibration differences and different X-values used (Table 3). It appears that most of the investigations cited in Table 4b, including the present one, do not include a correction for helium. The value quoted for Dame (1983) is smaller than his published value, because of his specific inclusion of a helium correction.

The results are consistent with arguments from authors who favour rough equality in the masses of the atomic and molecular components (Cesarsky et al., 1977; Blitz and Shu, 1980; Cohen et al., 1980; Li Ti pei et al., 1982; Lebrun et al., 1983; Dame, 1983; Thaddeus and Dame, 1984). We find that the H_2 mass even in the molecular ring exceeds the H I mass by only ~ 35 %. This value may be higher or lower at the peak of the ring depending on the true variation of X within the 2–8 kpc annulus. If molecular hydrogen is dominant over H I inside $R = 8$ kpc, we find that the dominance is weak, covering only a small fraction (15 %) of the surface area of the galaxy out to 20 kpc, the limiting distance for star formation and molecular clouds in the Milky Way.

Outside the solar circle, for $R < 15$ kpc, our results indicate that $M(H_2)$ is ~ 20 % of the total. The mass of H_2 we find outside the

solar circle of 2.3 $10^8\,M_\odot$ is consistent with the finding of Paper I, that H_2 can be neglected in analysing the gamma-ray emission from the outer Galaxy to at least the 10% level; the H I mass beyond $R=11$ kpc is found by Henderson et al. (1982) to be 4 $10^9\,M_\odot$. Finally, the values of X recently advocated by Bhat et al. (1985) are lower than ours by about 50%, but the discrepancy between their work and ours is largely a result of understated uncertainties in their analysis.

5.4. *Local gamma-ray emissivities*

The total gamma-ray emissivities at $R=10$ kpc, determined in Sect. 4.2 [$(0.96\pm0.08)\,10^{-26}$, $(0.72\pm0.05)\,10^{-26}$, and $(0.63\pm0.04)\,10^{-26}$ photon H atom^{-1} s^{-1} sr^{-1} for the 70–150 MeV, 150 MeV –300 MeV, and 300 MeV–5 GeV ranges], can be fitted by an $E^{-1.8}$ power-law spectrum. These emissivity values are in reasonable agreement with the local values found by Strong et al. (1982b) at intermediate latitudes ($10° \lesssim |b| \lesssim 20°$) from a comparison between COS-B data and Lick galaxy counts. However, the values show significantly better agreement with the improved emissivity values given by Strong (1985a) and Strong et al. (1985b), which were derived from a reanalysis of the intermediate-latitude regions using both galaxy counts and H I data and including IC emission. The values derived by Strong et al. (1985b) for the three energy ranges are: $(1.10\pm0.14)\,10^{-26}$, $(0.76\pm0.09)\,10^{-26}$, and $(0.68\pm0.09)\,10^{-26}$ photon H atom^{-1} s^{-1} sr^{-1}.

The determination of the local electron spectrum from gamma-ray emissivities, and the comparison with the spectrum derived from galactic non-thermal radio emission, requires a detailed evaluation as described by Gualandris and Strong (1984) and Strong (1985b). We limited ourselves to the easier reverse approach: calculation of the expected bremsstrahlung emissivities, for the three energy ranges analysed, from the radio electron spectrum. The expected bremsstrahlung spectrum $q(E_\gamma)$ for an electron spectrum of the form $I_e \propto E_e^{-\alpha}$ can be represented by:

$$q(E_\gamma) = \frac{K(E_\gamma,\alpha)}{E_\gamma} \int_{E_\gamma}^{\infty} I_e(E_e)\,dE_e, \qquad (5)$$

where the values of $K(E_\gamma,\alpha)$ are given by Gualandris and Strong (1984). Using the most recent determination of the electron spectrum ($E_e \gtrsim 70$ MeV, up to a few GeV; Webber, 1983), the bremsstrahlung emissivities were found to be $0.48\,10^{-26}$, $0.20\,10^{-26}$, and $0.10\,10^{-26}$ photon H atom^{-1} s^{-1} sr^{-1} for the 70–150 MeV, 150–300 MeV, and 300 MeV–5 GeV ranges, respectively. The bremsstrahlung contribution to our measured local gamma-ray emissivities follows from the results presented in Sect. 4.2 ($0.8 \leqq f \leqq 1.2$): $(0.38-0.57)\,10^{-26}$, $(0.20-0.38)\,10^{-26}$, and $(0.07-0.25)\,10^{-26}$ photon H atom^{-1} s^{-1} sr^{-1} for the same three energy ranges (the lower bound of the ranges corresponds to $f=1.2$, the upper bound to $f=0.8$), values in agreement with those given above. Gualandris and Strong (1984) found that the bremsstrahlung estimate from the gamma-ray emissivities for the 70–150 MeV range is a factor 1.5–2 times higher than the estimate from the Webber (1983) electron spectrum. With our lower total gamma-ray emissivity for the 70–150 MeV range (confirmed independently by the recent medium latitude study by Strong et al. (1985b), mentioned above) compared with the value used by Gualandris and Strong (1984), no discrepancy seems to be left (provided $f \gtrsim 1.1$) between the absolute intensities of the electron spectrum (around 100 MeV–1 GeV) derived from radio and gamma-ray observations, but if $f=1.0$ a factor of ~ 1.5 is still required.

5.5. *Comments on the CR distributions*

The extensions of the CR distributions (Sect. 4) to $R \lesssim 4$ kpc are uncertain because of the relatively small sky area ($l \lesssim 25°$) involved in the analysis of this part of the Galaxy. As a consistency check, the likelihood analysis described in Sect. 2 was also performed with two distance intervals for $R<8$ kpc: 2–5 kpc and 5–8 kpc. The gamma-ray emissivities in the two distance intervals were not found to be significantly different; in the 70–150 MeV range the emissivity value for the 2–5 kpc range is somewhat higher than for the 5–8 kpc range. We conclude that we have no indication of a concentration of cosmic rays around $R=5$–7 kpc, such as previous studies have claimed (see Sect. 5.7).

Although the gamma-ray observations and predictions are in good agreement, the longitude profiles presented in Fig. 5 also show some discrepancies, due partly to the presence of gamma-ray sources (e.g. in the Cygnus region and in the Carina region) that are either genuine point sources or localized enhancements of either the CR density or the H_2/CO ratio. In addition, CR enhancements that are expected in high density regions of spiral arms (Bignami and Fichtel, 1974), based on the theoretical considerations of Parker (1966, 1969), may account for some discrepancies (for instance for the interarm-region towards $l=65°$). However, all deviations are fairly small, and the large-scale CR distribution can be described by the exponential distributions determined in this paper; only weak modulations in high-density regions are possible.

5.6. *Comparison with synchrotron emission*

Independent information on the CR electron distribution can be obtained from the low-frequency radio-continuum emission that primarily results from interaction of CR electrons with the interstellar magnetic field. For an isotropic ensemble of relativistic electrons with differential spectrum $k \cdot E_e^{-\alpha}$, moving in a homogeneous magnetic field, the synchrotron emissivity is proportional to $k \cdot B_\perp^{(1+\alpha)/2}$, where $B_\perp$ is the field component perpendicular to the line of sight. The 408 MHz all-sky survey published by Haslam et al. (1981a, b) is most appropriate to a large-scale study. In a typical interstellar field of a few μG, the 408 MHz observations mainly trace electrons with energies of a few GeV, which is approximately an order of magnitude higher than the energy of the electrons that produce bremsstrahlung at gamma-ray energies of ~100 MeV.

Phillipps et al. (1981) and Kanbach (1983) both found from a radial unfolding of the 408 MHz survey that the galacto-centric distribution of the synchrotron volume emissivity in the galactic plane for $R \gtrsim 5$ kpc can be represented by an exponential distribution $e^{S_{syn}(R-R_\odot)}$, with $S_{syn}=-0.25\,\mathrm{kpc}^{-1}$. This distribution is steeper than the exponential CR electron distribution derived from the gamma-ray observations in Sect. 4 ($-0.21\,\mathrm{kpc}^{-1} < S_e < -0.09\,\mathrm{kpc}^{-1}$, for $0.8 \leqq f \leqq 1.2$, including 1σ uncertainties). Representing the radial distribution of the magnetic-field energy density ($\propto B^2$) also by an exponential distribution $e^{S_{mag}(R-R_\odot)}$, this incidates that $-0.19\,\mathrm{kpc}^{-1} < S_{mag} < -0.04\,\mathrm{kpc}^{-1}$. Following this approach the uncertainties are large, but a combined study of the low-frequency radio data, the gamma-ray data, and the H I and CO data, now available, may give further insight into the coupling among CR energy density (dominated by CR protons), energy density of the magnetic field, and gas density. Detailed investigations concerning the equilibrium (and stability) of the gaseous disk [similar to the studies of Kellman (1972), Fuchs et al. (1976), and Badhwar Stephens (1977)] are needed, but are beyond the scope of this paper.

5.7. Previous gamma-ray studies of the galactic CR distribution

Even though the importance of molecular hydrogen in the interpretation of gamma-ray observations was noted as early as 1975 by Stecker et al., up to now poor sky coverage of the CO observations severely limited the gamma-ray studies of the galactic CR distribution. In addition, the relation between the measured CO intensities and the H_2 column densities was highly uncertain. Making a virtue of necessity, the sparse CO observations, mostly concentrated on the mid plane of the Galaxy, and the 21-cm H I observations were usually converted into a galactic (spiral arm) model of the gas distribution. By assuming that the CR density on a large scale is proportional to the gas density, some studies showed that the observed and predicted gamma-ray intensities agree (e.g. Bignami et al., 1975; Kniffen et al., 1977; Fichtel and Kniffen, 1984) while others required modifications, such as abundance gradients or a partial exclusion of cosmic rays from molecular clouds (e.g. Cesarsky et al., 1977). Without making a priori assumptions on the proportionality between CR and gas density, several studies showed that the gamma-ray emissivity increases towards the inner parts of the Galaxy (e.g. Stecker et al., 1975; Higdon, 1979; Issa et al., 1981; Harding and Stecker, 1985). The conclusions were varied and highly uncertain. Using more and better data, which enables a more sophisticated analysis, the present work has overcome some of the difficulties that confronted earlier studies of the inner Galaxy.

For the outer Galaxy, the discrepancy between previous works using SAS-2 data (e.g. Dodds et al., 1975; Cesarsky et al., 1977; Higdon, 1979; Issa et al., 1981) and ours cannot be ascribed to uncertainties in the molecular-hydrogen contribution to the gamma-ray intensities, which is negligible (see Paper I and Sect. 5.3). The pioneering analysis of the gamma-ray data from the SAS-2 satellite by Dodds et al. (1975) first suggested a gradient in the density of CR nuclei in the outer Galaxy; that gradient has been adopted ever since as the main observational evidence against a universal origin of CR nuclei in the GeV range (see e.g. the review by Cesarsky, 1980). The disturbing disagreement with our findings in Papers I and II and in the present work, which all indicate a near constancy of the nuclei density throughout the entire Galaxy, seems, after all, to have a straightforward explanation: the gamma-ray intensities (>100 MeV) measured by the SAS-2 satellite, presented by Fichtel et al. (1975), and used by Dodds et al. (1975), are about a factor of 2 lower than the final outer-Galaxy intensities released by the SAS-2 group (Fichtel et al., 1978). This intensity difference may be ascribed to the improvement in calibration of SAS-2 after the first presentation of the data in 1975 (see Thompson et al., 1977); compare, for instance, the latitude and longitude profiles given by Dodds et al. (1975) with those of the final SAS-2 data presented by Hartman et al. (1979). Using these final SAS-2 data, we found that the "extra-galactic" model of Dodds et al. (i.e. a constant density of CR nuclei) predicts gamma-ray intensities that are even too low for the outer Galaxy, but, using recent estimates of the local gamma-ray emissivity for energies above 100 MeV (Sect. 5.4), which are $\sim 30\,\%$ higher than the value used by Dodds et al., we find good agreement.

It is not surprising, then, that other works (e.g. Cesarsky et al., 1977; Higdon, 1979) essentially confirmed the findings of Dodds et al.: they all relied on the same SAS-2 data base, presented by Fichtel et al. (1975). Using the final SAS-2 data, Strong et al. (1978), Arnaud et al. (1982), and Bloemen et al. (1984c) found no indication of a strong emissivity gradient (>100 MeV). Although Strong et al. (1978) and Arnaud et al. (1982) ascribed this result to a weaker gradient in the second galactic quadrant (which they studied) compared to the third quadrant, the disappearance of the strong gradient found by Dodds et al. (1975) is really due to the use of the recalibrated SAS-2 data.

Issa et al. (1981), analysing the final SAS-2 data and COS-B data, found a steep emissivity gradient outside the solar circle, independent of gamma-ray energy, but they used a radial-unfolding technique that gives highly uncertain results at the solar circle and is essentially inapplicable to regions beyond the solar circle. Recent work by Bhat et al. (1984) is largely based on this analysis by Issa et al. (1981). The local ($\lesssim$1 kpc) emissivity variation at medium latitudes ($|b|>10°$) discussed by Issa et al. (1981) and Bhat et al. (1984) can be ascribed solely to local variations in the electron density (Strong, 1985a; Strong et al., 1985b) that are beyond the scope of our large-scale analysis of the Milky Way.

6. Conclusions

A gamma-ray emissivity gradient as a function of galacto-centric radius is required to explain the COS-B gamma-ray observations in the integral 70 MeV–5 GeV range in terms of CR interactions with interstellar gas and photons. Using H I and CO observations to trace the gas distribution in the Galaxy, the gamma-ray model displays and energy dependence that cannot satisfactorily be ascribed to different emissivity spectra of H I and H_2 but can be accounted for fully by an energy-dependent galactic emissivity gradient that is strongest for low energies. The ratio $X = N(H_2)/W_{CO}$ is derived simultaneously in the likelihood fitting procedure of the gamma-ray observations and its value is found to be constant throughout the Galaxy, within the uncertainties of the analysis; $X = 2.75\ 10^{20}\,\mathrm{mol\cdot cm^{-2}\,K^{-1}\,km^{-1}\,s}$. The formal error is $0.35\ 10^{20}\,\mathrm{mol\cdot cm^{-2}\,K^{-1}\,km^{-1}\,s}$; taking into account our estimate of the total systematic uncertainty would probably increase this formal error by a factor of ~ 2. This X value should strictly be regarded as an upper limit if a population of unresolved galactic gamma-ray point sources distributed like CO exists. The resultant H_2 mass is equal to the H I mass for $2\,\mathrm{kpc} < R < 10\,\mathrm{kpc}$.

In terms of densities of CR electrons and nuclei, exponential CR distributions $e^{S(R-R_\odot)}$ as a function of galacto-centric radius R ($R_\odot = 10$ kpc) give an acceptable description of the gamma-ray observations. The value of S is in the range -0.21 to $-0.09\,\mathrm{kpc^{-1}}$ for CR electrons and -0.055 to $+0.015\,\mathrm{kpc^{-1}}$ for nuclei. A CR electron gradient is required, but the results are consistent with a constant density of CR nuclei on a galactic scale. The quoted CR gradients are upper limits if a population of unresolved galactic gamma-ray sources exists with a latitide distribution similar to that of the gas, but with a stronger concentration towards the inner parts of the Galaxy. If these sources would have a steeper spectrum compared to the diffuse gamma-ray emission, then a less steep electron gradient would be required.

The gradient in the distribution of the CR electrons confirms their galactic origin. As argued in Paper II, if the sources of electrons and nuclei are distributed similarly in the Galaxy, then extensive diffusion of the nuclei in the outer Galaxy would be required to reproduce the observed flat distribution; disk-confinement models will encounter difficulties, but also models involving a large halo (Ginzburg and Syrovatskii, 1964; Owens and Jokipii, 1977; Ginzburg et al., 1980) cannot be easily applied. The scale length of the nucleon component of cosmic rays from the present analysis is at least 15 kpc, much larger than for the type of objects generally considered as candidates for CR sources. For example, a recent determination of the distribution of pulsars

(Lyne et al., 1985) leads to a scale length of 5 kpc, and similar values are found for supernova remnants and young populations in general. Although propagation of cosmic rays is expected to widen the distribution of particles relative to their sources, this effect will depend strongly on the nature of the propagation geometry. Comparing the present distribution with the model of Strong (1977), in which 3-dimensional diffusion away from sources distributed like supernova remanants was assumed, the predicted variation is much too steep; this is an inevitable consequence of the rapid increase of the volume to be filled as the radius increases. If instead the propagation were essentially 2-dimensional, with particles diffusing in the plane much more rapidly than in the z-direction, the expected falloff with radius would be much less and essentially independent of the source distribution. Further pursuit of this problem is beyond the scope of this paper.

The gradient of the CR nuclei, if it exists, is so weak, that on the basis of gamma-ray observations, it is no longer certain that CR nuclei (with energies of several GeV) are produced in the Galaxy; the data are also consistent with an extra-galactic origin (Brecher and Burbidge, 1972; Burbidge, 1974). However, since weak modulations of the CR distribution due to high-matter-density regions might be present (Sect. 5e), at least part of the CR nuclei may have a galactic origin.

Acknowledgements. The Laboratory for Space Research Leiden is supported financially by the Netherlands Organisation for the Advancement of Pure Research (ZWO). This work was partially supported by grants no. 0407/83 from the NATO Scientific Affairs division and AST-8315276 from the U.S. National Science Foundation.

References

Arnaud, K., Li Ti pei, Riley, P.A., Wolfendale, A.W., Dame, T.M., Brock, J.E., Thaddeus, P.: 1982, *Monthly Notices Roy. Astron. Soc.* **201**, 745

Badhwar, G.D., Stephens, S.A.: 1977, *Astrophys. J.* **212**, 494

Bhat, C.L., Mayer, C.J., Wolfendale, A.W.: 1984, *Astron. Astrophys.* **140**, 284

Bhat, C.L., Issa, M.R., Houston, B.P., Mayer, C.J., Wolfendale, A.W.: 1985, *Nature* **314**, 511

Bignami, G.F., Fichtel, C.E.: 1974, *Astrophys. J. Letters* **189**, L65

Bignami, G.F., Fichtel, C.E., Kniffen, D.A., Thompson, D.J.: 1975, *Astrophys. J.* **199**, 54

Black, J.H., Willner, S.P.: 1984, *Astrophys. J.* **279**, 673

Blitz, L.:1980, in *Giant Molecular Clouds in the Galaxy*, eds. P.M. Solomon, M.G. Edmunds, Pergamon Press, Oxford, p. 1

Blitz, L., Shu, F.H.: 1980, *Astrophys. J.* **238**, 148

Blitz, L., Fich, M., Stark, A.A.: 1980, in *Interstellar Molecules*, ed. B. Andrew, Reidel, Dordrecht, p. 213

Blitz, L., Fich, M., Kulkarni, S.R.: 1983, *Science* **220**, 1233

Blitz, L., Magnani, L., Mundy, L.: 1984, *Astrophys. J.* **282**, L9

Blitz, L., Bloemen, J.B.G.M., Hermsen, W., Bania, T.M.: 1985, *Astron. Astrophys.* **143**, 267

Bloemen, J.B.G.M., Caraveo, P.A., Hermsen, W., Lebrun, F., Maddalena, R.J., Strong, A.W., Thaddeus, P.: 1984a, *Astron. Astrophys.* **139**, 37

Bloemen, J.B.G.M., Blitz, L., Hermsen, W.: 1984b, *Astrophys. J.* **279**, 136

Bloemen, J.B.G.M., Bennett, K., Bignami, G.F., Blitz, L., Caraveo, P.A., Gottwald, M., Hermsen, W., Lebrun, F., Mayer-Hasselwander, H.A., Strong, A.W.: 1984c, *Astron. Astrophys.* **135**, 12

Bloemen, J.B.G.M.: 1985, *Astron. Astrophys.* **145**, 391

Brecher, K., Burbidge, G.R.: 1972, *Astrophys. J.* **174**, 253

Brock, J.E. et al.: 1985 (in preparation)

Burbidge, G.R.: 1974, *Phil. Trans. Roy. Soc. Lond. A* **277**, 481

Burton, W.B., Gordon, M.A.: 1978, *Astron. Astrophys.* **63**, 7

Cesarsky, C.J., Cassé, M., Paul, J.A.: 1977, *Astron. Astrophys.* **60**, 139

Cesarsky, C.J., Völk, H.J.: 1978, *Astron. Astrophys.* **70**, 367

Cesarsky, C.J.: 1980, *Ann. Rev. Astron. Astrophys.* **18**, 289

Cohen, R.S., Thaddeus, P.: 1977, *Astrophys. J. Letters* **217**, L155

Cohen, R.S., Cong, H.I., Dame, T.M., Thaddeus, P.: 1980, *Astrophys. J.* **239**, L53

Cohen, R.S., Grabelsky, D.A., May, J., Bronfman, L., Alvarez, H., Thaddeus, P.: *Astrophys. J.* **290**, L15

Cohen, R.S., Dame, T.M., Thaddeus, P.: 1985b, *Astrophys. J. Suppl.* (in press)

Dame, T.M.: 1983, Ph. D. thesis, Columbia University

Dame, T.M., Thaddeus, P.: 1985, *Astrophys. J.* (in press)

Dickman, R.L.: 1978, *Astrophys. J. Suppl.* **37**, 407

Dodds, D., Strong, A.W., Wolfendale, A.W.: 1975, *Monthly Notices Roy. Astron. Soc.* **171**, 569

Eadie, W.T., Drijard, D., James, F.E., Roos, M., Sadoulet, B.: 1971, Statistical methods in experimental physics, North-Holland, Amsterdam, p. 230–232

Fazio, G.G.: 1967, *Ann. Rev. Astron. Astrophys.* **5**, 481

Fichtel, C.E., Hartman, R.C., Kniffen, D.A., Thompson, D.J., Bignami, G.F., Ögelman, H.B., Özel, M.E., Tümer, T.: 1975, *Astrophys. J.* **198**, 163

Fichtel, C.E., Hartman, R.C., Kniffen, D.A., Thompson, D.J., Ögelman, H.B., Tümer, T., Özel, M.E.: 1978, NASA Technical Memorandum 79650

Fichtel, C.E., Kniffen, D.A.: 1984, *Astron. Astrophys.* **134**, 13

Frerking, M.A., Langer, W.D., Wilson, R.W.: 1982, *Astrophys. J.* **262**, 590

Fuchs, B., Schlickeiser, R., Thielheim, K.O.: 1976, *Astrophys. J.* **206**, 589

Ginzburg, V.L., Syrovatskii, S.I.: 1964, The Origin of Cosmic Rays, Pergamon Press, Oxford

Ginzburg, V.L., Khazan, Y.M., Ptuskin, V.S.: 1980, *Astrophys. Space Sci.* **68**, 295

Gordon, M.A., Burton, W.B.: 1976, *Astrophys. J.* **208**, 346

Gualandris, F.L., Strong, A.W.: 1984, *Astron. Astrophys.* **140**, 357

Harding, A.K., Stecker, F.W.: 1985, *Astrophys. J.* **291**, 471

Hartman, R.C., Kniffen, D.A., Thompson, D.J., Fichtel, C.E., Ögelman, H.B., Tümer, T., Özel, M.E.: 1979, *Astrophys. J.* **230**, 597

Haslam, C.G.T., Klein, U., Salter, C.J., Stoffel, H., Wilson, W.E., Cleary, M.N., Cooke, D.J., Thomasson, P.: 1981a, *Astron. Astrophys.* **100**, 209

Haslam, C.G.T., Salter, C.J., Stoffel, H., Wilson, W.E.: 1981b, *Astron. Astrophys. Suppl.* **47**, 1

Heiles, C., Habing, H.J.: 1974, *Astron. Astrophys. Suppl.* **14**, 1

Heiles, C., Cleary, M.N.: 1979, *Australian J. Phys. Astrophys. Suppl.* **14**, 1

Henderson, A.P., Jackson, P.D., Kerr, F.J.: 1982, *Astrophys. J.* **263**, 182

Hermsen, W.: 1980, Ph.D. thesis, University of Leiden, The Netherlands

Higdon, J.C.: 1979, *Astrophys. J.* **232**, 113

Issa, M.R., Riley, P.A., Strong, A.W., Wolfendale, A.W.: 1981, *J. Phys. G* **7**, 973
Kanbach, G.: 1983, *Space Sci. Rev.* **36**, 273
Kellman, S.A.: 1972, *Astrophys. J.* **175**, 353
Kniffen, D.A., Fichtel, C.E., Thompson, D.J.: 1977, *Astrophys. J.* **215**, 765
Kulkarni, S.R., Blitz, L., Heiles, C.: 1982, *Astrophys. J.* **259**, L63
Kutner, M.L., Mead, K.: 1981, *Astrophys. J.* **249**, L15
Lebrun, F., Bennett, K., Bignami, G.F., Bloemen, J.B.G.M., Buccheri, R., Caraveo, P.A., Gottwald, M., Hermsen, W., Kanbach, G., Mayer-Hasselwander, H.A., Montmerle, T., Paul, J.A., Sacco, B., Strong, A.W., Wills, R.D., Dame, T.M., Cohen, R.A., Thaddeus, P.: 1983, *Astrophys. J.* **274**, 231
Lebrun, F., Huang, Y.-L.: 1984, *Astrophys. J.* **281**, 634
Li Ti pei, Riley, R.A., Wolfendale, A.W.: 1982, *J. Phys. G* **8**, 1141
Liszt, H.S., Xiang, D.-L., Burton, W.B.: 1981, *Astrophys. J.* **249**, 532
Liszt, H.S., Burton, W.B., Xiang, D.-L.: 1984, *Astron. Astrophys.* **140**, 303
Lyne, A.G., Manchester, R.N., Taylor, J.H.: 1985, *Monthly Notices Roy. Astron. Soc.* **213**, 613
Magnani, L., Blitz, L., Mundy, L.: 1985, *Astrophys. J.* **295**, 402
Mayer-Hasselwander, H.A., Bennett, K., Bignami, G.F., Buccheri, R., Caraveo, P.A., Hermsen, W., Kanbach, G., Lebrun, F., Lichti, G.G., Masnou, J.L., Paul, J.A., Pinkau, K., Sacco, B., Scarsi, L., Swanenburg, B.N., Wills, R.D.: 1982, *Astron. Astrophys.* **105**, 164
Mayer-Hasselwander, H.A.: 1983, in *Kinematics, Dynamics, and Structure of the Milky Way*, ed. W.L.H. Shuter, Reidel, Dordrecht, p. 223
Owens, A.J., Jokipii, J.R.: 1977, *Astrophys. J.* **215**, 677
Pagel, B.E.J., Edmunds, M.G.: 1981, *Ann. Rev. Astron. Astrophys.* **19**, 77
Parker, E.N.: 1966, *Astrophys. J.* **145**, 811
Parker, E.N.: 1969, *Space Sci. Rev.* **9**, 651
Penzias, A.A.: 1980, in *Interstellar Molecules*, Reidel, Dordrecht, p. 397
Phillipps, S., Kearsey, S., Osborne, J.L., Haslam, C.G.T., Stoffel, H.: 1981, *Astron. Astrophys.* **98**, 286
Pollock, A.M.T., Bennett, K., Bignami, G.F., Bloemen, J.B.G.M., Buccheri, R., Caraveo, P.A., Hermsen, W., Kanbach, G., Lebrun, F., Mayer-Hasselwander, H.A., Strong, A.W.: 1984, *Astron. Astrophys.* **146**, 352
Rockstroh, J.M., Webber, W.R.: 1978, *Astrophys. J.* **224**, 677
Sanders, D.B., Solomon, P.M., Scoville, N.Z.: 1984, *Astrophys. J.* **276**, 182
Sanders, D.B., Scoville, N.Z., Solomon, P.M.: 1985, *Astrophys. J.* **289**, 373
Scoville, N.Z., Solomon, P.M.: 1975, *Astrophys. J.* **199**, L105
Solomon, P.M., Sanders, D.B.: 1980, in *Giant Molecular Clouds in the Galaxy*, eds. P.M. Solomon, M.G. Edmunds, Pergamon Press, Oxford, p. 41
Skilling, J., Strong, A.W.: 1976, *Astron. Astrophys.* **53**, 253
Stecker, F.W.: 1971, Cosmic Gamma Rays, Mono Book Corp., Baltimore
Stecker, F.W., Solomon, P.M., Scoville, N.Z., Ryter, C.E.: 1975, *Astrophys. J.* **201**, 90
Stephens, S.A., Badhwar, G.D.: 1981, *Astrophys. Space Sci.* **76**, 213
Strong, A.W.: 1977, *Monthly Notices Roy. Astron. Soc.* **181**, 311
Strong, A.W., Wolfendale, A.W., Bennett, K., Wills, R.D.: 1978, *Monthly Notices Roy. Astron. Soc.* **182**, 751
Strong, A.W., Riley, P.A., Osborne, J.L., Murray, J.D.: 1982a, *Monthly Notices Roy. Astron. Soc.* **201**, 495
Strong, A.W., Bignami, G.F., Bloemen, J.B.G.M., Buccheri, R., Caraveo, P.A., Hermsen, W., Kanbach, G., Lebrun, F., Mayer-Hasselwander, H.A., Paul, J.A., Wills, R.: 1982b, *Astron. Astrophys.* **115**, 404
Strong, A.W.: 1985a, *Astron. Astrophys.* **145**, 81
Strong, A.W.: 1985b, in *Proc. 19th Int. Cosmic Ray Conf.*, OG 3.1–7
Strong, A.W., Bloemen, J.B.G.M., Lebrun, F., Hermsen, W., Mayer-Hasselwander, H.A.: 1985a, *Astron. Astrophys. Suppl.* (submitted)
Strong, A.W., Bloemen, J.B.G.M., Hermsen, W., Mayer-Hasselwander, H.A.: 1985b, in *Proc. 19th Int. Cosmic Ray Conf.*, OG 3.1–3
Strong, A.W., Bloemen, J.B.G.M., Buccheri, R., Hermsen, W., Lebrun, F., Mayer-Hasselwander, H.A.: 1985c, in *Proc. 19th Int. Cosmic Ray Conf.*, OG 9.3–9
Swanenburg, B.N., Bennett, K., Bignami, G.F., Buccheri, R., Caraveo, P.A., Hermsen, W., Kanbach, G., Lichti, G.G., Masnou, J.L., Mayer-Hasselwander, H.A., Paul, J.A., Sacco, B., Scarsi, L., Wills, R.D.: 1981, *Astrophys. J.* **243**, L69
Thaddeus, P., Dame, T.M.: 1984, in *Occasional Reports Royal Observatory*, Edinburgh, No. 13, p. 15
Thompson, D.J., Fichtel, C.E., Kniffen, D.A., Ögelman, H.B.: 1977, *Astrophys. J.* **214**, L17
Wannier, P.G.: 1980, *Ann. Rev. Astron. Astrophys.* **18**, 399
Weaver, H., Williams, D.R.W.: 1973, *Astron. Astrophys. Suppl.* **8**, 1
Webber, W.R., Simpson, G.A., Cane, H.V.: 1980, *Astrophys. J.* **236**, 448
Webber, W.R.: 1983, in *Composition and Origin of Cosmic Rays*, ed. M.M. Shapiro, Reidel, Dordrecht, p. 83